

COPYRIGHT WARNING

This paper is protected by copyright. You are advised to print or download **ONE COPY** of this paper for your own private reference, study and research purposes. You are prohibited having acts infringing upon copyright as stipulated in Laws and Regulations of Intellectual Property, including, but not limited to, appropriating, impersonating, publishing, distributing, modifying, altering, mutilating, distorting, reproducing, duplicating, displaying, communicating, disseminating, making derivative work, commercializing and converting to other forms the paper and/or any part of the paper. The acts could be done in actual life and/or via communication networks and by digital means without permission of copyright holders.

The users shall acknowledge and strictly respect to the copyright. The recitation must be reasonable and properly. If the users do not agree to all of these terms, do not use this paper. The users shall be responsible for legal issues if they make any copyright infringements. Failure to comply with this warning may expose you to:

- Disciplinary action by the Vietnamese-German University.
- Legal action for copyright infringement.
- Heavy legal penalties and consequences shall be applied by the competent authorities.

The Vietnamese-German University and the authors reserve all their intellectual property rights.



Methodology for Automated Graph Model Creation and Customer Allocation to Enhance Gas Quality Tracking Efficiency

Bachelor thesis



Submitted by Tu Tuan Tran

Mat.-Nr. 108020266047

VGU ID: 16644

Study subject: Mechanical Engineering

Submission date: 27.12.2023

1st Supervisor: Dr. Peter Schley (SmartSim GmbH)

2nd Supervisor: Prof. Dr.-Ing. Roland Span (RUHR-UNIVERSITÄT BOCHUM)

Declaration of independence

I hereby certify that I have written this Bachelor thesis independently and exclusively with the sources or aids indicated in the bibliography. This encompasses potential graphical representations and tabular data. I have identified and attributed all excerpts and sentences within my research that have been borrowed from either published or unpublished works, clearly citing their precise origins. It is important to note that this thesis has not been previously submitted, either by me or any other individual, to any other academic authority for evaluation in a comparable form.

Tran, Tu Tuan

Name, First name



Vung Tau, 26/12/2023

Place, date, signature



Vietnamese-German University

Blocking Note

This bachelor thesis contains confidential data of SmartSim GmbH and EWE NETZ GmbH. Publication, duplication of the thesis, or other disclosure to third parties – even in part – is not permitted without the written consent of SmartSim GmbH and EWE NETZ GmbH. The bachelor thesis is to be made accessible only to examiners as well as members of the examination board.

Acknowledgements

This thesis was written following my internship at SmartSim GmbH during my exchange semester in Germany. I express genuine gratitude for the invaluable support and assistance provided during the period of composing this thesis, acknowledging the contributions of those individuals who support me in facilitating this endeavor.

I express my foremost gratitude to Dr. Peter Schley, Ms. Inka Stinn, and Mr. Henning Markgraf for their supervision of my thesis. Their invaluable explanations, suggestions, and feedback throughout the entire period have guided this thesis in the right direction.

I would like to extend my appreciation to all my colleagues at SmartSim GmbH for fostering a welcoming and professional working environment. Their friendliness and helped me overcome cultural barriers, contributing to a delightful working experience.

Lastly, I extend my gratitude to Prof. Dr.-Ing. Roland Span and Ms. Tan Trieu Giang Nguyen for their invaluable assistance, ensuring a comfortable experience during my study and stay in Germany.



Abstract

The implementation of gas quality tracking necessitates a series of manual steps, introducing the potential for errors and requiring significant effort, depending on the complexity of projects and networks. This thesis addresses two key objectives. The first involves the creation of a graph model to serve as an input topology for the implementation of gas quality tracking with SmartSim software. The second objective is the allocation of customers within the lower-pressure grid to regulators. The thesis explores alternative approaches for this allocation based on volume distribution, discussing various methodologies. To investigate these approaches, an analysis of factors influencing volume distribution will be conducted.

Table of figures

Figure 1: Standardized Daily Energy Consumption dependence on temperature.	15
Figure 2: Example graph model of a gas grid.....	17
Figure 3: Generate graph model based on GIS data.....	19
Figure 4: Result of mapNearestNodes Tool.....	26
Figure 5: SLP Volume distribution of “Northern Coastal” section by mapNearestNodes	29
Figure 6: Lowest pressure within section in relation to temperature.....	31
Figure 7: The proportion of outlet points exceeding 1.79 bar in relation to temperature.	32
Figure 8: Temperature – dependent volume flow through Gustow and Garz regulators.....	33
Figure 9: Temperature – dependent volume distribution in various injection pressure pairs	34
Figure 10: Absolute volume of Gustow–Garz section by mapNearestNodes & regulator measurements	35
Figure 11: Volume distribution of Gustow – Garz section by mapNearestNodes & STANET & measurements	36
Figure 12: Daily pressure at Gustow and Garz regulators	38
Figure 13: Volume distribution of Gustow–Garz section by mapNearestNodes & STANET at equal injection pressure (1.8 bar).....	39
Figure 14: Volume distribution from SmartSim, dynamic node weights, and equally weighted nodes.....	40
Figure 15: Area supplied by Gustow, Garz regulators at same pressure.....	44
Figure 16: Rügen central section	45
Figure 17: Volume flow through Prora and Binz Heizkraftwerk regulators.....	46
Figure 18: Gustow - Garz section.....	58
Figure 19: SLP & RLM volume shares in Rügen' sections in 2022.....	61

Table of Contents

Declaration of independence.....	1
Blocking Note.....	3
Acknowledgements.....	4
Abstract.....	5
Table of figures	6
1. Introduction	9
1.1. Motivation.....	9
1.2. Scope of the thesis.....	9
1.3. Structure of the thesis.....	10
2. Fundamentals.....	11
2.1. Gas quality tracking.....	11
2.1.1. Definition of the gas distribution networks.....	11
2.1.2. The SmartSim software.....	12
2.1.3. Description of standard load profile (SLP) procedure	14
2.2. Representation of a gas grid	15
2.2.1. Graph model of a gas grid in SmartSim	15
2.2.2. Gas grid representation in GIS.....	17
3. Methodology.....	19
3.1. Creation of a graph model of a gas grid.....	19
3.2. Allocation of customers	21
3.2.1. mapNearestNodes Tool	24



3.2.2.	STANET static simulation of lower pressure grid.....	26
4.	Results and discussion	28
4.1.	The influences of different factors on the volume distribution	28
4.1.1.	Temperature influence on volume distribution	28
4.1.2.	Sensitivity analyses with STANET.....	30
4.2.	Comparison of different volume distributions	34
4.3.	Derivation of node weights.....	40
5.	Summary and Outlook	47
6.	Bibliography	50
7.	Appendixes.....	52
7.1.	Appendix A: Create Graph Model with QGIS Python Console.....	52
7.2.	Appendix B: Rügen SLP profiles and their distribution in analyzed section	57
7.3.	Appendix C: SLP & RLM volume shares in Rügen' sections	61

1. Introduction

1.1. Motivation

The European gas market is growing more dynamic due to the merging of national markets. Europe is witnessing increased imports of liquefied natural gas (LNG) and the harmonization of technical regulations, which eases natural gas trade across borders. Additionally, the rising use of renewable energies, like biogas and hydrogen from power-to-gas plants, is contributing to fluctuations in gas quality and calorific value[1]. Gas grid operators are confronted with challenges in accurately calculating energy supply to end customers despite varying gas qualities.

Exit volumes in regional distribution networks are typically not subject to measurement. Consequently, gas quality tracking emerged as a method to determine calorific values, crucial in determining flow conditions across the grid through flow mechanics calculations. Within the scope of this thesis, the SmartSim software will be employed as the designated method for gas quality tracking, wherein exit volumes are gauged through the application of standard load profiles (SLP) as outlined by Hellwig [2], coupled with a novel correction algorithm developed by Schley et al.[3]–[5]. The application of gas quality tracking, specifically SmartSim software frequently eliminates the necessity for intricate measurement tools or the use of propane gas conditioning.

Overall, the implementation of gas quality tracking necessitates the creation of a topology model suitable for grid simulations and the allocation of customers to the inject points of the regional distribution grid. Currently, this process involves a series of manual steps, which, depending on the network's complexity, not only introduces the risk of errors but also demands substantial effort. Therefore, it is imperative to devise a solution that minimizes manual labor within this procedure.

1.2. Scope of the thesis

Within the scope of this study, a methodology is developed for standardizing and automating the creation of a graph model of the gas grid utilizing a Geographical Information System (GIS) and subsequent allocation of customers to this model. Diverse approaches pertaining to customer allocation will be thoroughly explored and assessed. The outcomes of this thesis' endeavor are

anticipated to make a substantial contribution to enhancing the efficiency and precision of gas quality tracking.

1.3. Structure of the thesis

Following this introductory chapter, Chapter 2 will delve into the theoretical foundations of gas quality tracking, which will encompass elucidating key concepts such as the definition of a gas distribution network, the utilization of gas quality tracking through SmartSim software, a portrayal of the Standard Load Profile (SLP) procedures; followed by the description of the setup of a graph model for a gas distribution network.

In Chapter 3, a comprehensive examination of the processes involved in graph model of the gas grid and customer allocation will be presented. An alternative approach to streamline the allocation procedure, employing node weights for volume distribution, will also be described upon.

Chapter 4 will focus on conducting a sensitivity analysis on the factors influencing volume distribution and will compare various methods for establishing node weights. The conclusion of this chapter will provide guidelines for the establishment of node weights.

Chapter 5 will serve as a conclusion of the thesis results, addressing the methodologies employed in the creation of node weights. Challenges encountered during this process will be discussed, and recommendations for enhancing the procedure will be proposed.

2. Fundamentals

2.1. Gas quality tracking

Gas quality tracking serves as an alternative method for ascertaining the calorific value used for billing end customers within a supply area characterized by multiple sources of natural gas, biogas, or hydrogen. As per the guidelines outlined in DVGW Code of Practice G 685[6], the utilization of substitute techniques to calculate the superior calorific value is permitted when the cost-effective implementation of advanced metering technology in distribution networks is unfeasible. This circumstance is typically encountered in local and regional distribution networks, particularly at the outlet points of local networks where volume meters are absent[6]. The subsequent sections will offer detailed insights into the gas supply network under consideration for the analysis, an exploration of the operation of SmartSim software in tracking gas quality, as well as the fundamentals of the application of standard load profile (SLP) method.

2.1.1. Definition of the gas distribution networks

Germany's natural gas supply system comprises transport networks and regional as well as local distribution networks, linked through network interconnection points (NKP). The transport network handles the long-distance transportation of natural gas at pressures of 80 bar and features well-established metering infrastructure at entry and exit points with limited interconnections. Exits lead to downstream (regional) distribution networks, major consumers like gas power plants, and natural gas storage facilities via metering and control stations.

The downstream regional distribution networks operate at pressures ranging from 4 bar to 30 bar and exhibit varying meshed networks with incomplete metering infrastructure at the regulators to the lower pressure grid. The outflow towards downstream local distribution networks, major consumers, or industrial clients occurs through measuring and control stations. Typically, large or industrial customers have their own measurement device, and are referred to as RLM customers, which stands for "Registrierte Leistungsmessung" in German.

Downstream local networks supply towns and (large) cities at operating pressures between 20 mbar and 1 bar above ambient pressure. These local distribution networks are characterized by limited metering infrastructure and intricate meshed or branched topologies. Small consumers within the local network only have annual meter readings. To determine monthly, daily or hourly energies from the yearly consumption, the standard load profile procedure is used. Such customers are referred as SLP customers [7], [8].

The assigning of customers to entry points for this analysis takes place within the local network supply in which both RLM and SLP customers are located.

2.1.2. The SmartSim software

The SmartSim software simulates the gas qualities within distribution networks. Taking into account a set of input data, it computes the flow conditions and the mixing of different gases within representation of the gas grid. Consequently, the calorific values at all exit points of the grid are trackable from the measured entry calorific values and the simulation. The following sections elaborate on the necessary input data for employing calculation on the SmartSim software[7].

2.1.2.1. Input Data

The initial prerequisite is the creation of a graph model that defines the network's topology. This model includes both the geographical data and the interconnections of nodes, pipes, valves, and regulators. Additionally, the topology data encompasses non-spatial information essential for storing physical attributes of pipes, such as their length, diameter, and roughness. The concept of the graph model of SmartSim topology is further discussed in 2.2.

In addition to the graph model of the grid, the simulation requires a dataset with hourly resolution. This dataset must include data on the calorific values, standard density, CO₂ content, volume flow rates and pressure at injection points. These quality of input data follow calibration regulations. The volume flow rates at exit points for unmeasured customers are derived from the SLP profiles, more details in 2.1.3. The customer values for each load profile are aggregated at the exit nodes. The data for both RLM and SLP consumers must be assigned to the correct exit nodes [7], [9].

Presently, the process of allocating SLP customers to the exit points varies considerably across individual projects. The specifics of these procedures will be outlined in 3.2.

2.1.2.2. Output Data

In practice, the calculations are performed on a monthly basis, with hourly calorific values being calculated for each exit point. Following the guidelines set out in DVGW worksheet G685[6], the monthly average calorific value for each exit point is calculated as follows:

$$HS_m = \frac{\sum_{i=1}^L HS_h(i) \cdot Vn_h(i)}{\sum_{i=1}^L Vn_h(i)} \quad (2.1)$$

HS_m , the superior calorific value HS on a monthly basis (index m)

HS_h , the superior calorific value HS on an hourly basis (index h)

Vn_h , the volume in standard state Vn on hourly basis

i , the running index hour 1 to L

L , number of hours of the month

In the case of a single exit point injecting in a calorific value district, also termed as single sided feed-in, the calculated mean value HS_m is the billing nominal value $HS_{m,eff}$.

$$HS_{m,eff} = HS_m \quad (2.2)$$

In the case of multiple exit points injecting into a calorific value district, also termed as multi-lateral feed-in, a volume weighted calorific value must be calculated for the CV district [7], [9]. The invoiced calorific value $HS_{m,eff}$ results from the volume weighted averaging over the N exit nodes in the calorific value district follows the DVGW worksheet G685' guideline for multi-lateral feed-in[6].

$$HS_{m,eff} = \frac{\sum_{i=1}^N HS_m(i) \cdot Vn_m(i)}{\sum_{i=1}^N Vn_m(i)} \quad (2.3)$$

$HS_{m,eff}$, the billing calorific value HS_{eff} on monthly basis (index m)

HS_m , the feed in calorific value HS on a monthly basis

Vn_m , the volume in standard state Vn on monthly basis

i , the running index exit points 1 to N

N , the number of exit points

2.1.3. Description of standard load profile (SLP) procedure

Considering the liberalization of the gas market, particularly to ensure the fair distribution of gas quantities from all suppliers through network operators' gas networks, a simplified approach of billing small customers was devised. While upgrading the metering infrastructure for small customers in residential and commercial/retail/service sectors was deemed economically unfeasible[10], in 2002, the Chair of Energy Economics and Application Technology at the Technical University of Munich developed a streamlined statistical method for estimating gas quantities for typical customer groups without the need for load profile measurements. This work was carried out on behalf of the Federal Association of the German Gas and Water Industry (BGW) and the Association of Municipal Companies (VKU). The standard load profile method involves breaking down the consumption from the previous meter reading period into smaller time units. This approach strikes a balance between the research effort needed for consumer data and the accuracy of the mathematical approximation. The essential data required are limited to customer type, annual consumption, and climatic location[2].

2.1.3.1. Calculation of the load profiles

The anticipated consumption pattern of customers is defined by a sigmoid function, which calculates the standardized daily energy usage, denoted as $h(\vartheta)$, based on the daily average temperature ϑ [11].

$$h(\vartheta) = \frac{A}{1 + \left(\frac{\vartheta - 40^\circ\text{C}}{B}\right)^C} + D \quad (2.4)$$

The parameters A, B, C, and D in the formula are determined using historical measurements obtained from various load profile categories, such as single-family houses, apartment buildings, or different retail sectors.

The hourly energy consumption E_h is calculated as the result of multiplying the standardized energy usage $h(\vartheta)$, the daily factor F_d , the hourly factor F_h , and the customer-specific value E_c .

$$E_h(h, d, \vartheta) = E_c \cdot F_h(h) \cdot F_d(d) \cdot h(\vartheta) \quad (2.5)$$

The factor F_d acknowledges variations in consumption patterns between weekdays and weekends. The factor F_h considers that energy usage varies depending on the time of day. The customer value E_c represents a standardized hourly energy consumption.

2.1.3.2. Customer profile types

The customer groups considered are divided into categories from the household and commercial/trade/service sectors[12]. The customer profile types, their annotations can be seen in 7.2, and their dependencies on temperature is illustrated in Figure 1.

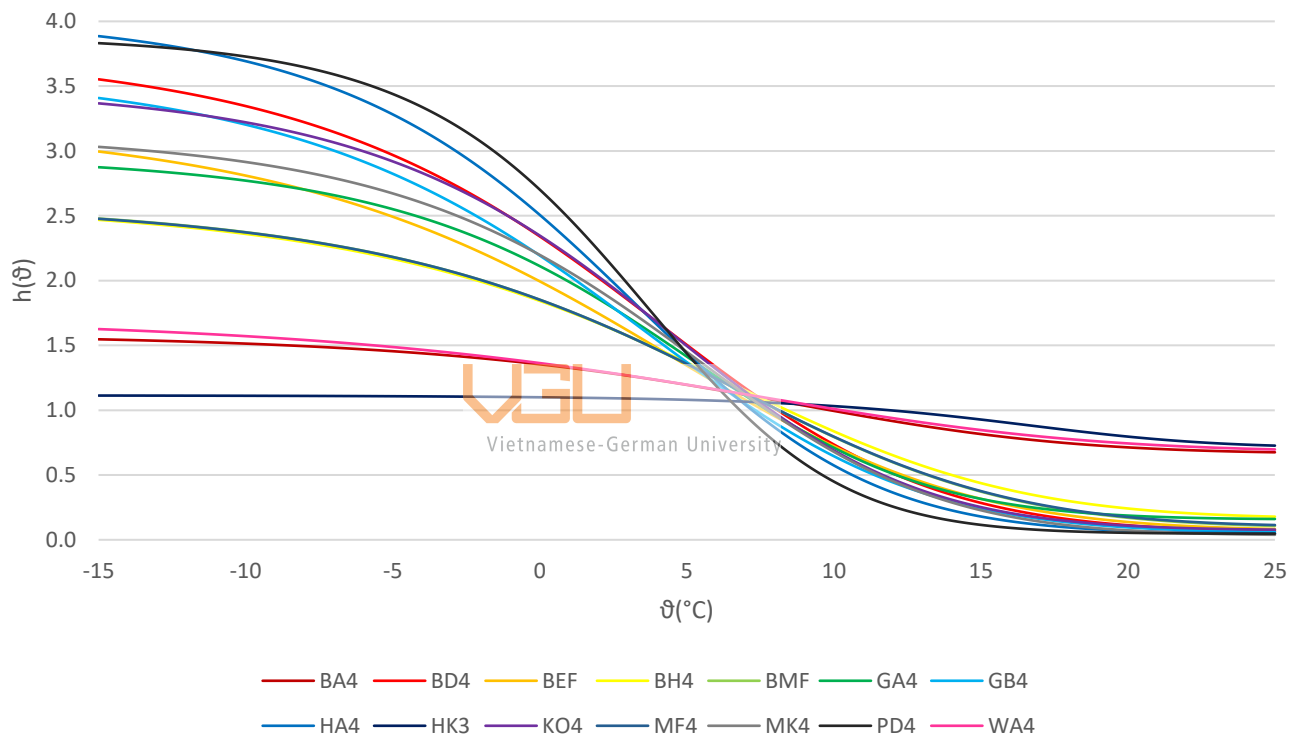


Figure 1: Standardized Daily Energy Consumption dependence on temperature.

With the environment temperature measured in daily resolution, the standardized energy consumption $h(\theta)$ is calculated, it is then multiplied with the hourly factor F_h , daily factor F_d of the profile and the customer value E_c , which derived from the past records, to estimate the energy consumption of a SLP customer on an hourly basis.

2.2. Representation of a gas grid

2.2.1. Graph model of a gas grid in SmartSim

In SmartSim, the gas quality tracking system used for this thesis, mathematical graph theory is employed to model the network. In this framework, the entities are represented as vertices, also referred to as nodes or points, while their connections are illustrated by edges, also known as lines. The spatial configuration of these vertices and edges within the graph provides a structured and visual representation, aiding in a clear comprehension of the relationships among these entities.

Hielscher and Vollmer outlined fundamental rules and key terminologies relevant to gas grid modeling [7], [8]. The gas grid consists of discrete grid elements that interconnect to constitute a grid section, each defined by two vertices: a start vertex and an end vertex. These vertices, referred to as nodes, encompass entry nodes and exit nodes. Gas is introduced into the grid through entry nodes and exits via exit nodes, with connections between grid elements exclusively taking place at non-entry/exit nodes. Gas flow is confined to these connection points, facilitating the ingress or egress of gas within the grid elements.

The major grid element, known as pipelines, is characterized by three physical attributes: length, diameter, and roughness of the pipe. It's noteworthy to mention that these parameters are considered constant for each individual pipe during the gas grid modeling process. Among the grid elements, pipelines uniquely possess the capability to store gas, which is termed as line pack, and transport gas. A pipeline is deemed terminated under certain conditions, including a notable alteration in pipe parameters (length, diameter, and roughness), the presence of another entry or exit node, or the occurrence of a branching event.

Other grid elements include valves, volume flow regulators, pressure regulators, and compressors. These components play a crucial role in defining boundary conditions for analyzing the flow dynamics within the grid. Valves, in particular, have the ability to partition a gas grid into distinct grid sections, resulting in what is termed "hydraulic separation," where specific sections are entirely isolated from others within the modeled grid or when grid operators deliberately deactivate the regulators for a specific duration.

The complete graph model of a gas grid is exemplified in Figure 2, where the node marked in red signifies the entry point. This model incorporates two regulators facilitating the flow of gas from the regional network (characterized by higher pressure) to the local distribution network (characterized by lower pressure). In the SmartSim software, a local distribution network supplied by two or more regulators, as exemplified here, is categorized as a section. This categorization is noteworthy, as these sections follow distinct procedures for gas quality tracking in contrast to a single-feed local network.

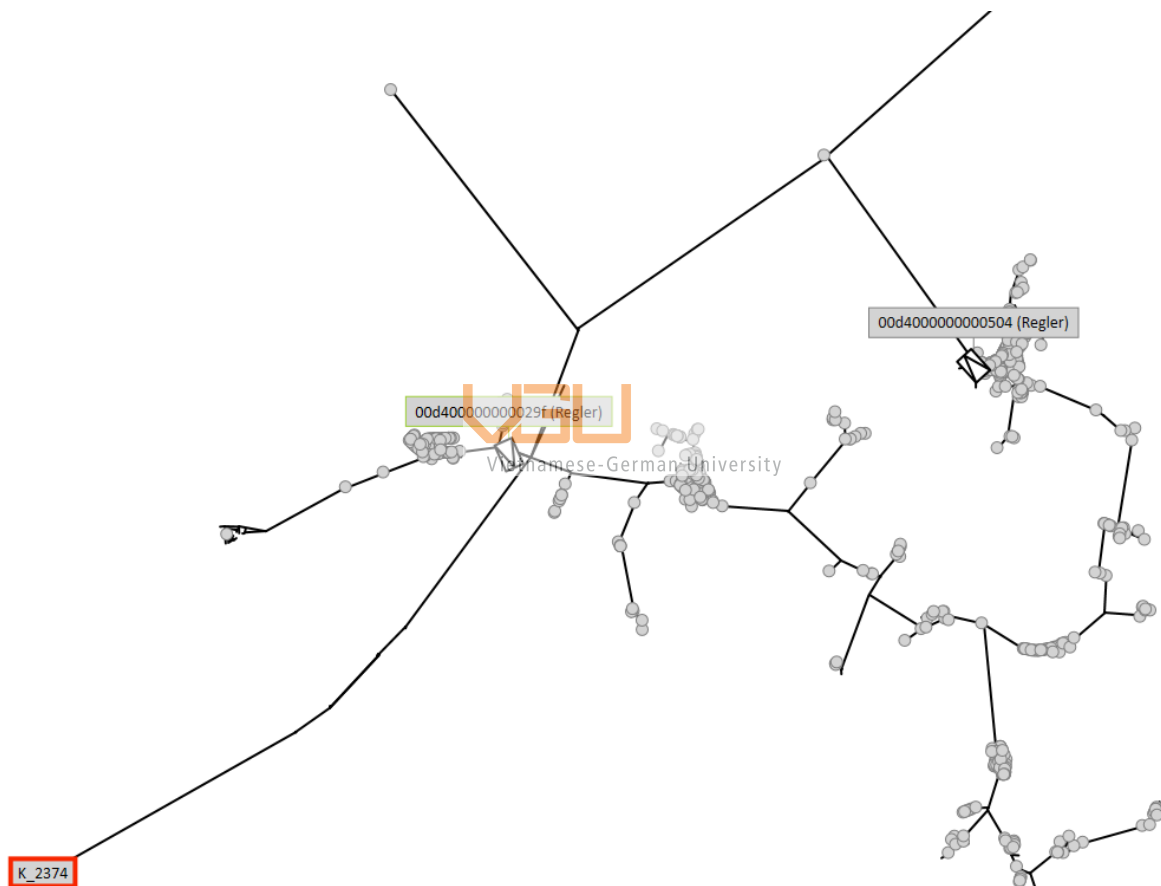


Figure 2: Example graph model of a gas grid

2.2.2. Gas grid representation in GIS

A Geographic Information System (GIS) is a computerized tool designed to acquire, store, validate, and present information pertaining to Earth's geographical locations. It has the capability to integrate diverse data types, for example streets, structures, and infrastructures, onto a singular map.

This integration facilitates enhanced visualization, analysis, and comprehension of various patterns and interconnections for users [13].

GIS serves a role in the efficient management of gas distribution networks by enabling oversight of essential assets. This encompasses creating a comprehensive inventory and visually representing vital components such as pipelines, valves, meters, and associated infrastructure. The digital representation of these assets within GIS facilitates advanced spatial analysis, thereby enhancing decision-making processes of the network renovation.

For the purpose of this thesis, QGIS, an open-source geographic information system (GIS) software that facilitates the creation, manipulation, visualization, analysis, and management of geospatial data will be used. Notably, this software provides a wide array of tools that are well-suited for the creation of the SmartSim input topology as a graph model.

3. Methodology

This thesis will establish the graph model of SmartSim topology based on the gas grid Rügen. Once the topology is defined, it will be utilized to inspect various methodologies for deriving node weights which involves SmartSim calculations.

3.1. Creation of a graph model of a gas grid

The digital information of a gas grid, obtained from grid operators, may exhibit variations across projects. However, a common classification for this information is GIS data. To make it compatible with SmartSim as input topology, this GIS data needs to undergo a transformation into a graph model. Within QGIS software, the digital positions of grid elements stored in GIS data is categorized as geometry data. This allows for subsequent translation into Well Known Text (WKT), a text markup language specifically designed for representing vector geometry objects. These formats were initially outlined by the Open Geospatial Consortium [14], the process of transforming geospatial information of pipes into a graph model is presented in Figure 3. In this depiction, the pipe, having undergone conversion, is now defined by its start and end nodes. Importantly, the coordinates of the edge, previously stored in the WKT format, are presently indicated by the corresponding node elements.

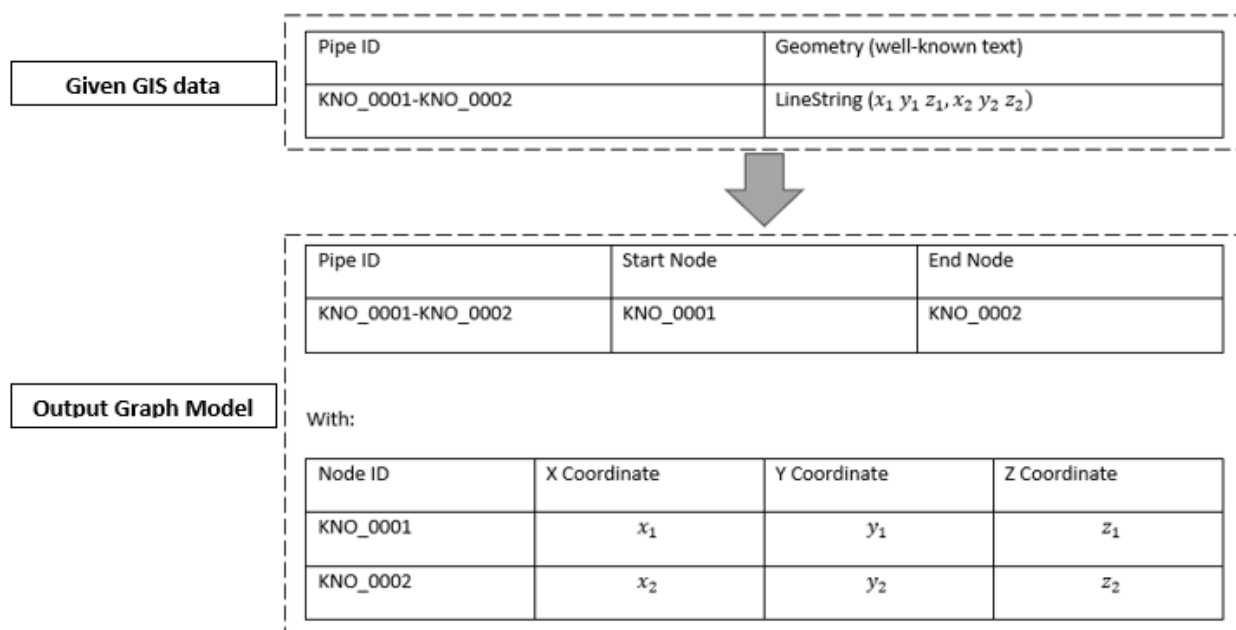


Figure 3: Generate graph model based on GIS data.

To derive a graph model based on the provided GIS network data obtained from grid operators, the following steps have been undertaken.

1. Define the Coordinate Reference System (CRS) of the Project:

Selecting the accurate CRS is paramount, as an incorrect choice can distort maps and misrepresent real-world features. Employing standard and appropriate CRSs for the mapped area is essential to uphold precision and consistency throughout the process.

2. Validate Connectivity within the Pipe Network:

While GIS data serves various purposes, spatial analysis and geographical information calculations necessitate precise input to generate an accurate graph model of the grid. Ensuring connectivity within the pipe network is vital for these calculations.

3. Create the Graph Model from Validated Topology:

Once the quality and precision of the topology have been assured, a series of integrated built-in tools within QGIS software can be employed to generate a graph model from the validated topology. The specific coding details for this process will be provided in 7.1.

4. Determine the Topology parts for simulation inclusion:

Considering the complexity of the local distribution gas grid, including all provided assets in the simulation can reduce efficiency without significantly enhancing calculation results. In most cases it is sufficient to include the high pressure level of the grid. For the majority of the lower pressure grids, they are reduced and represented by exit points and referred as sub-grids. It's crucial to carefully decide which parts of the topology to incorporate for an efficient simulation.

5. Identify entry nodes, exit nodes, regulators, and valves:

The different assets in the GIS data have to be translated to the grid elements of a SmartSim topology mentioned in 2.2.1 – nodes, pipes, vales and regulators. Entry points denote locations where gas is introduced into the network, and this information is provided by the grid operator. Valves, one of the grid components, exert influence over the flow within the network by either allowing or blocking gas flow. Regulators, on the other hand, represent line objects connecting higher-pressure grids to lower-pressure grids.

Exit nodes mark the outlets of the network, essentially representing the points where consumers extract gas from the networks. For the sub-grids, which are not included in the simulation, exit nodes are pinpointed by the starting point of regulators that

provide input to the respective sub-grids. These nodes serve as proxies for the actual exit points, the customers which are not encompassed in the final SmartSim topology.

6. Determine sections:

Upon identification of exit points and regulators, situations may arise where two or more inlets coexist within a lower-pressure grid or when the sub-grid is represented by two or more exit points. In such instances, the sub-grid or lower-pressure grid is categorized as a section. This classification is vital for the calculation of gas quality values in a multi-lateral feed-in calorific value district, as outlined in 2.1.2.2.

While the creation of graph models can be automated using the software's built-in tools, there are additional steps that require human involvement to validate, enhance the topology's quality, and to reduce the sub – grids. These steps depend significantly on the given data and the complexity of the gas grid under consideration. Once these steps are accomplished, the topology graph model is ready to be implemented.

3.2. Allocation of customers

For the sub-grids that are not included in the SmartSim topology, the consumption of the SLP and RLM customers within the sub-grid accumulates to the corresponding exit point. This aggregation of customer consumption requires their association with the respective exit node. This is trivial in sub – grids, which can be represented by only one exit point. In sub-grids classified as sections, as determined in step 6 discussed in 3.1, which have multiple feed-in regulators and need representation by more than one exit point, the distribution of total consumption in the sub-grid to different exit points poses challenges. Currently, a definitive guideline for this process is absent, one way of modelling the distribution is to employ so-called node weights for all exit nodes of a section. For each feed point i to a local network section, the outlet volume V_i with the consideration of node weight w_i is calculated as follows:

$$V_i = w_i \cdot \sum_{section} V_{consumer} \quad (3.1)$$

The objective of this thesis is to explore methodology for generating node weights and to examine the general approach of incorporating node weights.

A straightforward approach to node weighting involves evenly distributing the total volume among all exit points within a section, known as the equally weighted exit node method.

Another alternative approach is utilizing the volume distribution calculated from different sources to derive node weights. The Rügen grid has the access to multiple methods to obtain volume flow into section, which are the volume flow through regulator measured with turbine meters with 4% claimed by the grid operator, the definitive information of lower pressure grid to set up static simulation with STANET, mentioned in 3.2.2. The volume flow into section can also be calculated by aggregating customers consumption to the nearest exit node by the mapNearestNodes tool, further detailed in 3.2.1. Under the assumption that the consumption trends remain relatively stable in the subsequent years, the volume distribution calculated through these methods will be then used as a reference to set up the node weight for the following years. Node weights derived from this method is now then addressed as fixed node weights.

Taking into account that profiles and temperature also influence volume distribution, as discussed later in 4.1.1, the derivation of node weight can be modified to incorporate temperature as an input for calculating node weight. Building on the results of the mapNearestNodes tool combined with the consumption estimated via SLP methods, mentioned in 2.1.3.1, node weight can be established without employing any simulation. These node weights obtained from this method are now referred to as dynamic node weights.

Given the distinct behaviors of RLM customers compared to SLP profiles and acknowledging variations within the RLM customer category, some of them may significantly impact the volume flow in the section. Consequently, mapping these customers to a single exit point becomes questionable. Due to the individual specificity of RLM customers for the purpose of establishing general dynamic node weights, the measured volume of RLM customers is not considered when establishing node weights.

According to the guidelines set out in DVGW worksheet G685 about billing calorific value in multi – lateral feed – in calorific value district [6], often referred as a section in this study, customers

within a section shares the same invoiced calorific value. As a result, the customers volume consumption, calculated by dividing the energy consumption to the calorific value, is proportional to the energy consumption. This, in turn, leads to the volume distribution being equal to the energy distribution.

Based on the equation 2.5 for the hourly energy consumption of SLP customers, while the input temperature ϑ remains constant throughout the day and the sum of the hourly factors of a day is one, the daily energy consumption E_d can be calculated as follow:

$$E_d = E_C \cdot F_d(d) \cdot h(\vartheta) \cdot \sum_{\text{hours of day}} F_h(h) = E_C \cdot F_d(d) \cdot h(\vartheta) \quad (3.2)$$

Dynamic node weights should be derived on a daily basis to be responsive to both temperature, daily factor, and eliminate the effect of hourly factor. The daily weight w_d , which derived from aggregate customers is established as follows:

$$w_d = \sum_{\text{SLP profiles}} h_{\text{profile}}(\vartheta) \cdot F_{d,\text{profile}}(d) \cdot \sum_{\text{customers}} E_{C,\text{profile}} \quad (3.3)$$

Overall, the mapNearestNodes method distributes the customers in a grid to the nearest regulator, thus only considering the physical properties of pipes and customer locations. This approach assumes an ideal scenario where the pressures at the regulators of a section would be identical. In real-world situations, injection pressure and temperature exert significant influences on the volume distribution, especially the temperature is the main factor that determines the gas demands from the SLP customers. To analyze the impact of this influence on the volume distribution at the regulators and thus node weights, a sensitivity analysis was carried out with STANET for the regulator pressures and the environment temperature.

In this study, SmartSim serves as the designated simulation software to evaluate the outcomes generated by the mapNearestNodes tool, node weights, equally weighted nodes. Concurrently, STANET stationary simulation is employed as a reference to observe and analyze the flow behavior under varied input conditions, such as pressure and temperature, which may not be explicitly captured in recorded data.

3.2.1. mapNearestNodes Tool

The mapNearestNodes tool was written in Python by SmartSim and exclusively used within the company. This tool utilizes the dijkstra_path_length function from NetworkX package, which uses Dijkstra's method to compute the shortest weighted path length between two nodes in a graph[15]. By inputting two lists of 'origin nodes' and 'target nodes', it becomes feasible to ascertain the nearest exit point (target node) for each customer (origin node). In this context, "closest" refers to the node with the smallest sum of weights within the graph model. The weighting factor of a pipe was derived from Darcy–Weisbach equation for pressure loss in a cylindrical pipe of uniform diameter D [16]:

$$\frac{\Delta p}{L} = f_D \cdot \frac{\rho}{2} \cdot \frac{\bar{v}^2}{D_H} \quad (3.4)$$

Where the pressure loss per unit length $\frac{\Delta p}{L}$ (SI unit: Pa/m) is the function of:

ρ , the density of the fluid (kg/m^3).

D_H , the hydraulic pressure of the pipe, in this context this equal to D (m).

\bar{v} , the mean flow velocity (m/s^2).

f_D , the Darcy Friction factor.

While the mean flow velocity \bar{v} can be derived as the volumetric flow rate Q per unit cross sectional area A , the Darcy-Weisbach equation for pressure loss can be rewritten as follows:

$$\Delta p = f_D \cdot \frac{\rho}{2} \cdot \frac{Q^2}{A^2} \cdot \frac{1}{D} \cdot L = f_D \cdot \frac{\rho}{2} \cdot \frac{Q^2}{\left(\pi \cdot \frac{D^2}{4}\right)^2} \cdot \frac{1}{D} \cdot L = f_D \cdot \frac{8 \cdot \rho \cdot Q^2}{\pi^2} \cdot \frac{L}{D^5} \quad (3.5)$$

Exclude the external parameters $\frac{8 \cdot \rho \cdot Q^2}{\pi^2}$ and simplify the impact of the diameter and roughness of the pipe in the calculation of the Darcy coefficient f_D , the weighting factor of the pipe for a fixed volume flow, gas and pipe roughness is determined by a simplified relation based on the pipe length L and the diameter D :

$$w = \frac{L}{D^5} \quad (3.6)$$

With the employment of the tool, the result of mapping customers to Exit points is visualized in Figure 4. Customers are represented by round dots positioned within polygons, symbolizing the sections. Purple lines illustrate the pipes in SmartSim topology, green lines depict the pipe in the sub-grids, and the thin colored lines connect the customers and the exit points, which they are mapped to. The Rügen grid consists of a total of five sections, each incorporating exit points as outlined in the Table 1.

Section	Exit points
Central	Kluis, Samtens, Sehlen, Bergen Süd, Bergen Heizwerk, Putbus, Binz Heizkraftwerk, Prora
Northern Coastal	Trent, Sagard, Mukran
Sassnitz	Sassnitz Lancken, Sassnitz Dwaasieden
Gustow – Garz	Gustow, Garz
Göhren – Sellin	Göhren, Sellin

Table 1: Rügen sections and their exit points

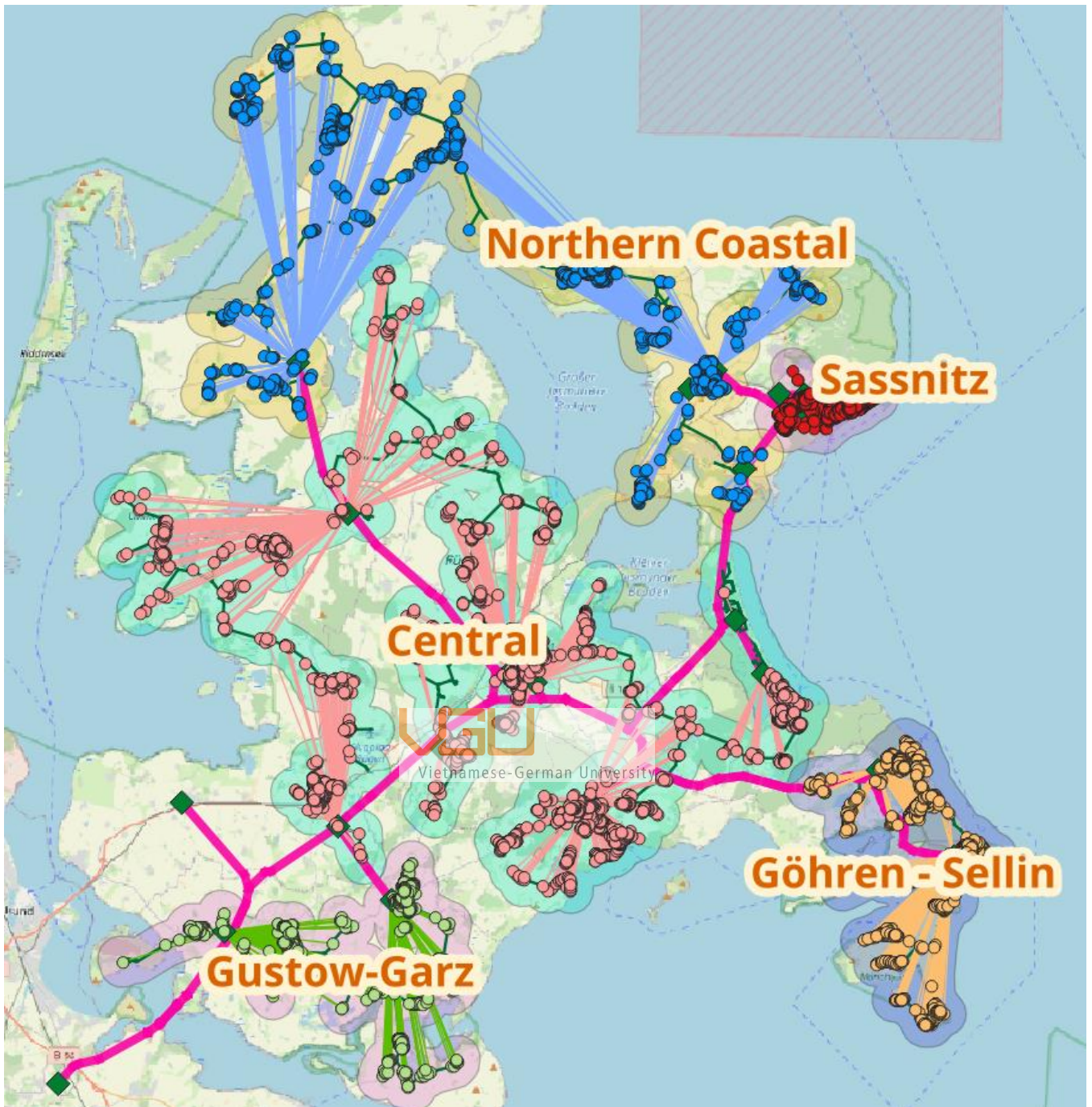


Figure 4: Result of mapNearestNodes Tool

3.2.2. STANET static simulation of lower pressure grid

STANET is a software designed for both stationary and dynamic assessments of supply and distribution networks. In this thesis, STANET is applied for stationary calculations of the sub-grids, in order to perform a sensitivity analysis for the input variables pressure and temperature. In this stationary analysis, STANET leverages input parameters, including the pressure at the two regulators,

environment temperature, and the date of calculations. These parameters, combined with the volume flow data from the previous year—consisting of recorded RLM consumption and SLP volumes—are integral to the simulation. The SLP volumes are calculated by dividing the last year's energy consumption, estimated through SLP methods, by the average higher calorific value determined with SmartSim. This comprehensive dataset is then utilized to simulate the gas flow within the section. This simulation facilitates a thorough examination of the gas flow through regulators of the section.

4. Results and discussion

In this chapter, the influences of regulators' injection pressure and environmental temperature on volume distribution are discussed. Once the influences are clarified, they are then employed to explain the difference between the aggregated consumption via the mapNearestNodes tool and the volume calculated through simulating the section with STANET. The volume flow through the regulator measured with turbine meters and is taken as a reference for the results. Taking all into account, a guideline for the derivation of node weight is then discussed.

4.1. The influences of different factors on the volume distribution

Within this section, we conduct an analysis of the influence of SLP profiles on volume distribution using the SmartSim software. Additionally, this chapter examines the effects of air temperature and the pressure at the regulator outlets on the flow through the regulators of a section. Air temperature is the main influence to the gas consumption in a section. The differences in injection pressures at the regulators within a section constitutes another significant influence. This examination is undertaken through the application of STANET simulation of the lower – pressure grid which is classified as a section.

Given that a RLM customer exhibits distinct behaviors compared to SLP profiles, and is individually specific in RLM customer category, this analysis primarily focuses on SLP customers. The Gustow – Garz section of the Rügen grid exclusively comprises SLP customers, more details in 7.3, making it a suitable case for examining the different impacts on the SLP customers and comparison between the volume distribution obtained from different methods. For analyses of sections that do not use measured volume as a reference, the aggregation of volume using mapNearestNodes will be performed exclusively with SLP volume. The section involved in these analyses is the “Northen Coastal” section.

4.1.1. *Temperature influence on volume distribution*

As depicted in Figure 1, showcasing standardized daily energy consumption of SLP profiles in response to temperature variations, the majority exhibit a notable sensitivity to temperature

changes—increasing with rising temperatures and decreasing with falling temperatures. Notably, HK3, BA4, and WA4 align with this general trend in responding to temperature; however, they stand out as exceptions due to their reactions being less pronounced than those observed in other profiles. These profiles, associated with cooking gas (HK3), bakery (BA4), and laundry services (WA4), demonstrate a consistent demand for gas, remaining higher than other profiles during temperature increases and not exhibiting a significant increase during temperature decreases.

This behavior contributes to a notable shift in volume distribution, particularly evident in the “Northern Coastal” section at the Mukran exit point. While the allocation of the bakery (BA4) profile to other exit points is either low or non-existent, there is a notably higher share of this profile associated with the Mukran exit point, more details in 7.2. Figure 5 depicts a notable surge in the Mukran share during summer months, marked by high temperatures, in contrast to colder months like December or January. This leads to a significant 2.59% variation, representing a 39.3% relative difference in the share of the "Mukran" exit point in July compared to December.

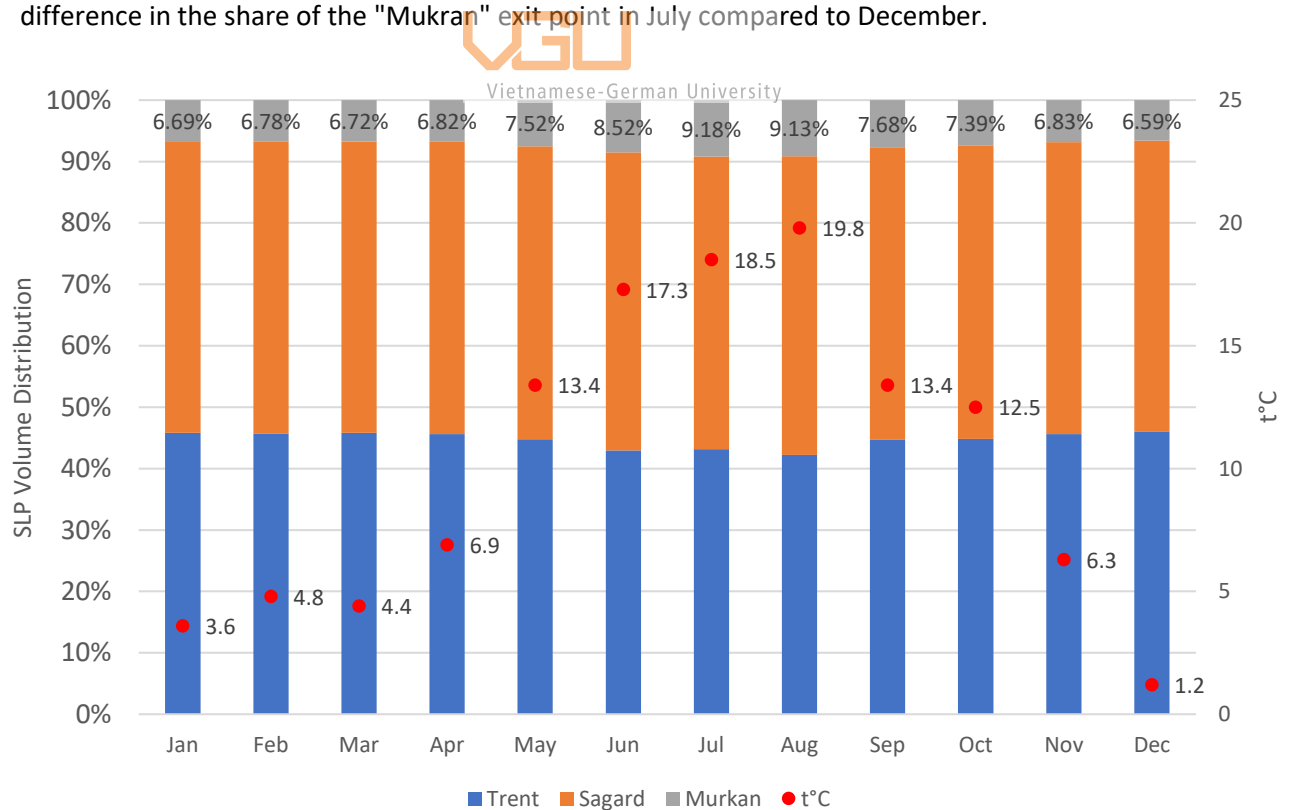


Figure 5: SLP Volume distribution of “Northern Coastal” section by mapNearestNodes

During high-temperature months, the demand for gas from other profiles experienced a notable decrease, whereas the bakery (BA4) profile exhibited a less pronounced influence by temperature changes. Conversely, in December, a period of low temperatures, while other profiles increased their gas demands, the bakery (BA4) profile did not show a significant increase.

4.1.2. Sensitivity analyses with STANET

As outlined in section 2.1.3.1, the energy consumption of a customer estimated by the SLP method is temperature dependence due to the standardized daily energy consumption. Despite all the distinct behavior of profile types in Figure 1, all profiles experience a reduction in consumption as temperature increases.

Volume consumption plays a pivotal role in influencing the pressure drop across the grid. Illustrated in Figure 6 are the lowest pressures calculated with STANET within the section as the temperature incrementally rises from -15°C to 25°C in 5°C intervals, with input pressures recorded as 1.8 bar at Gustow and 1.79 bar at the Garz regulator. As the temperature rises, there is a direct correlation with a decrease in consumption within the section, the lowest pressure in the section increases. In other words, the pressure drop in the section diminishes with rise in temperature. This is attributed to the decrease in volume consumption of SLP customers as temperatures increase, resulting in reduced volume flow and consequently a decrease in pressure drop within the section. The behavior is described by the relation of volume flow and pressure drop in Darcy Weisbach equation mentioned in 3.2.1. Notably, at temperatures of 20°C and 25°C, the lowest pressure in the grid exceeds the threshold of 1.79 bar at the Garz regulator.

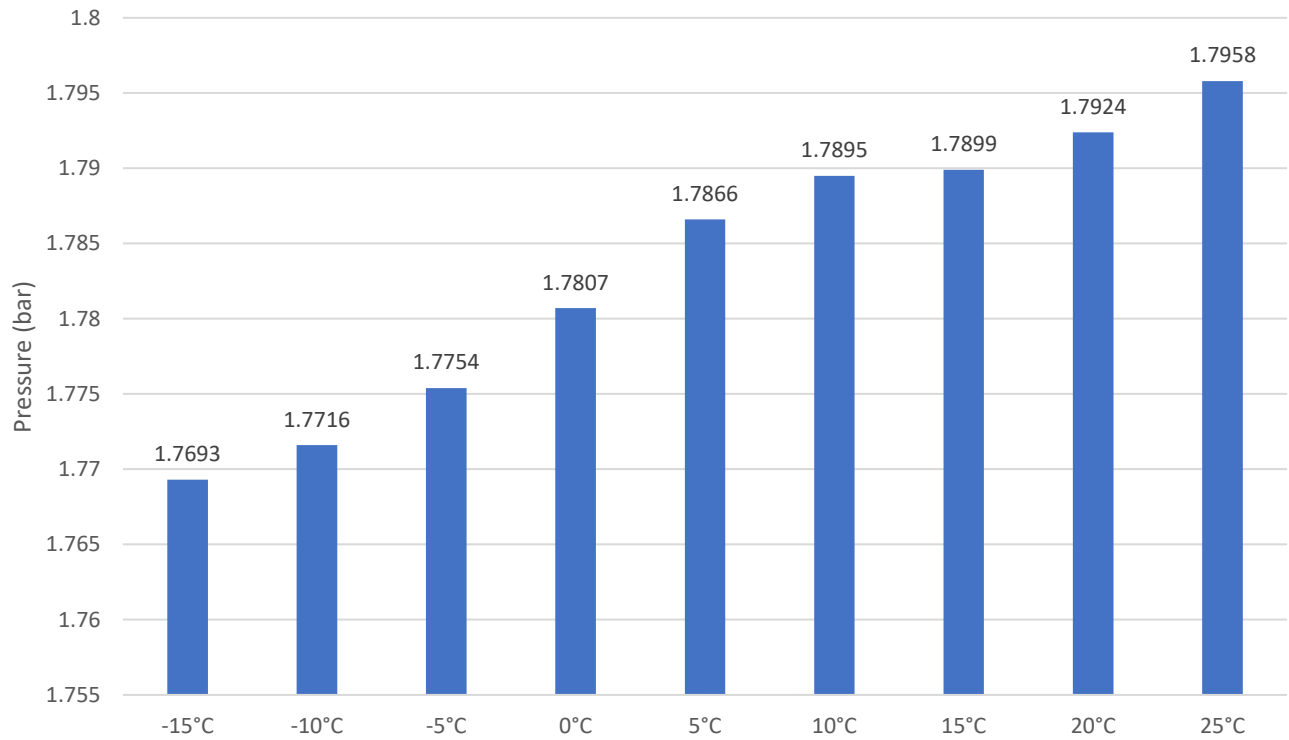


Figure 6: Lowest pressure within section in relation to temperature

The pressure drops within the section are visually represented in Figure 7, depicting the percentage of outlet points where the pressure exceeds the 1.79 bar threshold at the Garz regulator. As shown in the diagram, with an increase in temperature, there is a corresponding rise in the proportion of outlet nodes exceeding the 1.79 bar threshold. Notably, at 20°C and 25°C, all outlet pressures surpass the 1.79 bar threshold.

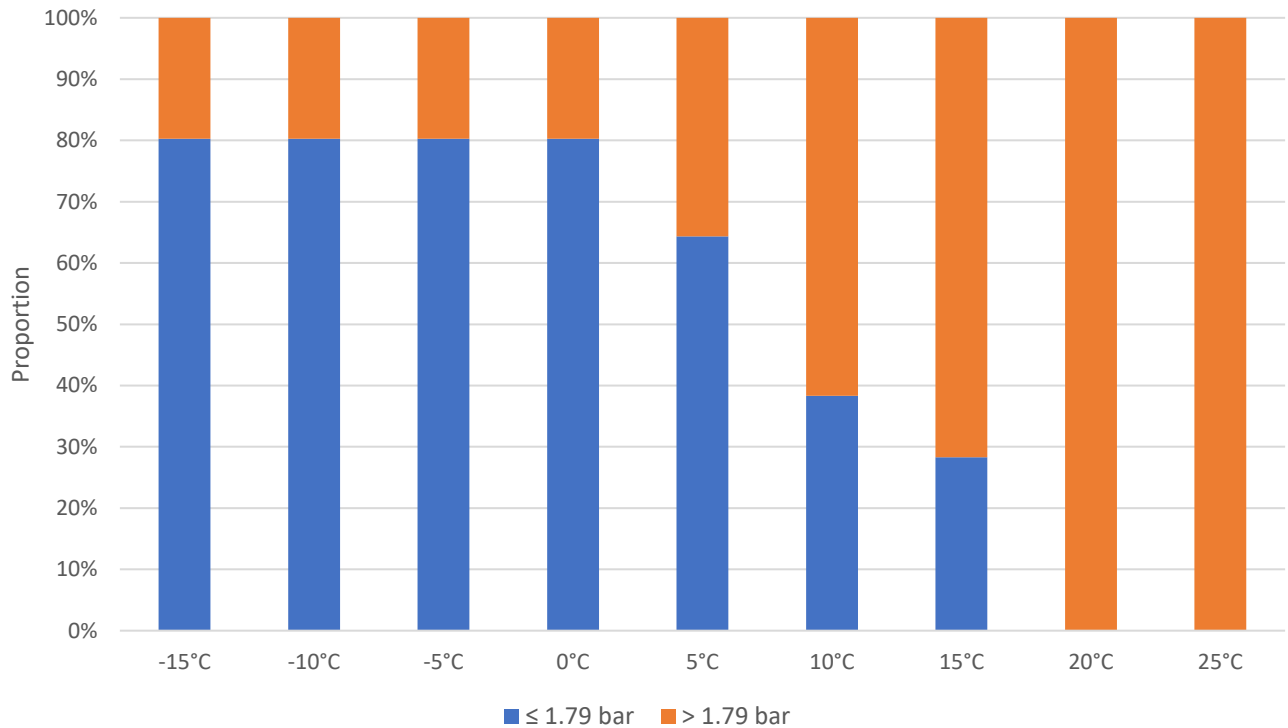


Figure 7: The proportion of outlet points exceeding 1.79 bar in relation to temperature.

Since gas cannot flow from high pressure to low pressure, the supply of gas through the Garz regulator is blocked from the outlets where pressure is higher than 1.79 bar. The effect of this to the volume distribution can be seen in Figure 8 , which illustrates the hourly volume flow (in m³) to the section via the regulators as temperature increases.

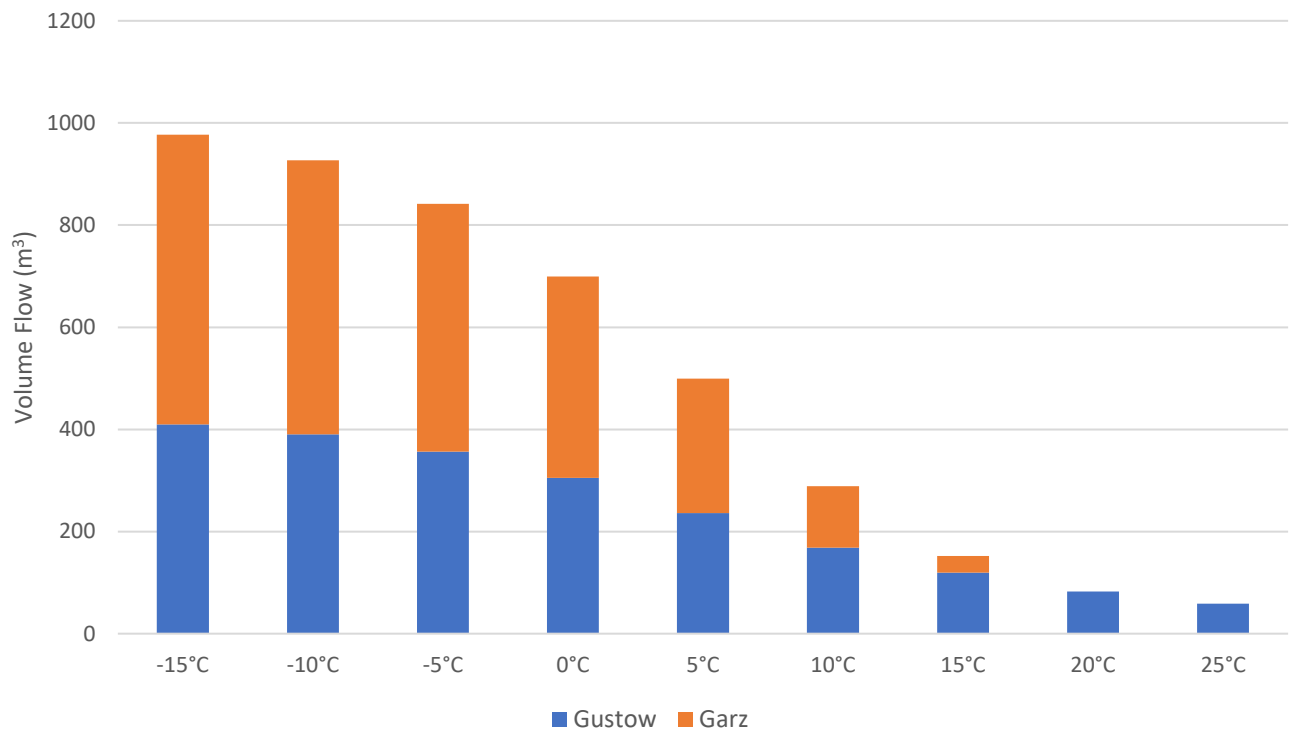


Figure 8: Temperature – dependent volume flow through Gustow and Garz regulators.

In addition to the initial injection pressure pair ($p_{\text{Gustow}}/p_{\text{Garz}}$) set at (1.8 bar/1.79 bar), various simulations with different pressure pairs were conducted to assess the sensitivity of injection pressure to volume distribution. The pressure pairs were derived from the measured pressure data in 2022 at the Gustow and Garz regulators, serving as references. The pressures exhibit a range between 1.78 bar and 1.82 bar, with a mean difference of 0.00575 bar, as illustrated in Figure 12. The results of these simulations are illustrated in Figure 9.

For the low temperature range from -15°C to 0°C, the volume distribution remains similar across various injection pressure pairs. However, at higher temperatures (15°C and above), significant changes in volume distribution occur, trending towards regulators with higher injection pressure. Notably, within the same injection pressure setup, the volume distribution remains stable across the temperature range.

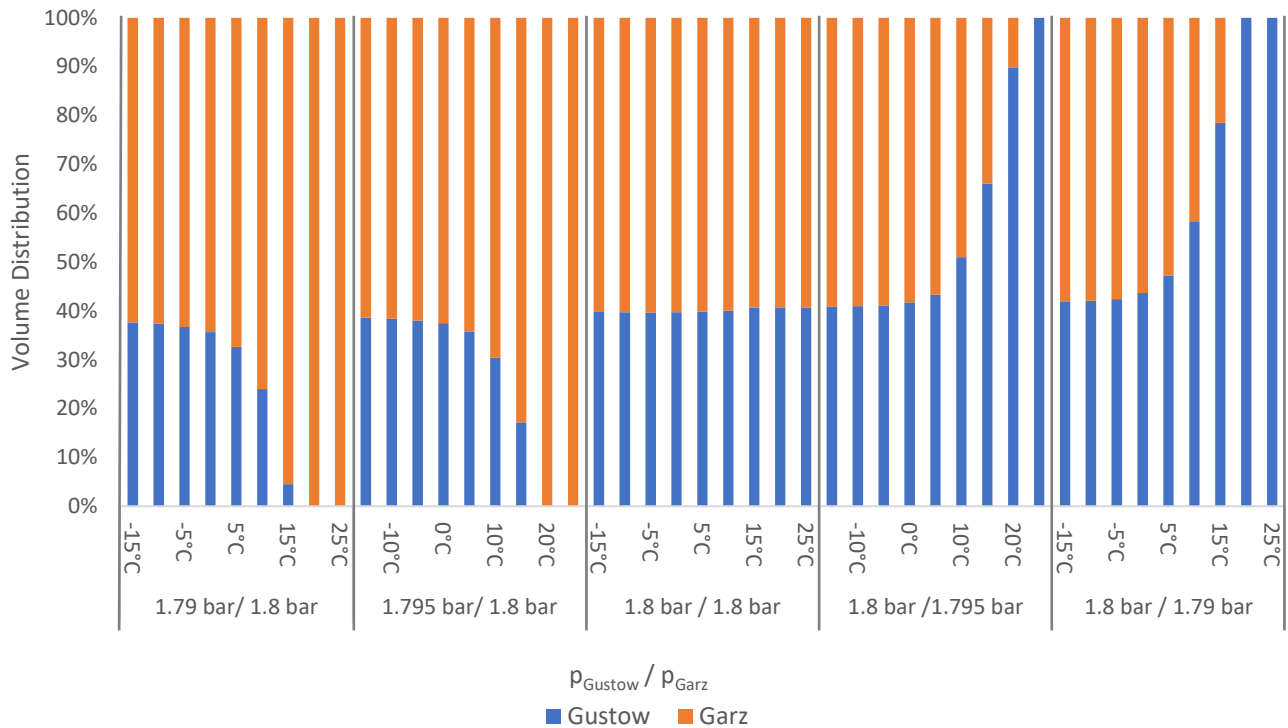


Figure 9: Temperature – dependent volume distribution in various injection pressure pairs

4.2. Comparison of different volume distributions

The Rügen gas grid is one of the rare grids with several available options for calculating volume distribution through regulators. Firstly, volume flow measurements through the regulators provided by the grid operator and there are well-defined GIS data for lower pressure grids, which may be absent in some projects. This section aims to compare volume distribution in the "Gustow – Garz" section between the three methods – customer assignment to exit point using the mapNearestNodes tool, measured volume, and static simulation with STANET.

Figure 10 depicts the aggregated SLP volume using the mapNearestNodes tool and the actual volume flow from the measurements through the regulators. Despite inherent uncertainties in estimating SLP customer consumption, the total volume flow into the Gustow – Garz section, as computed by SmartSim software, closely aligns with measurements obtained through field devices in most months, excluding May to October. Beside the high uncertainties of SLP volumes, discrepancies in alignment during these months may be attributed to the turbine meter used for measurement,

which encounters challenges at low flow rates. Turbine meters typically have a start-up or minimum flow rate below which accurate measurements become difficult.

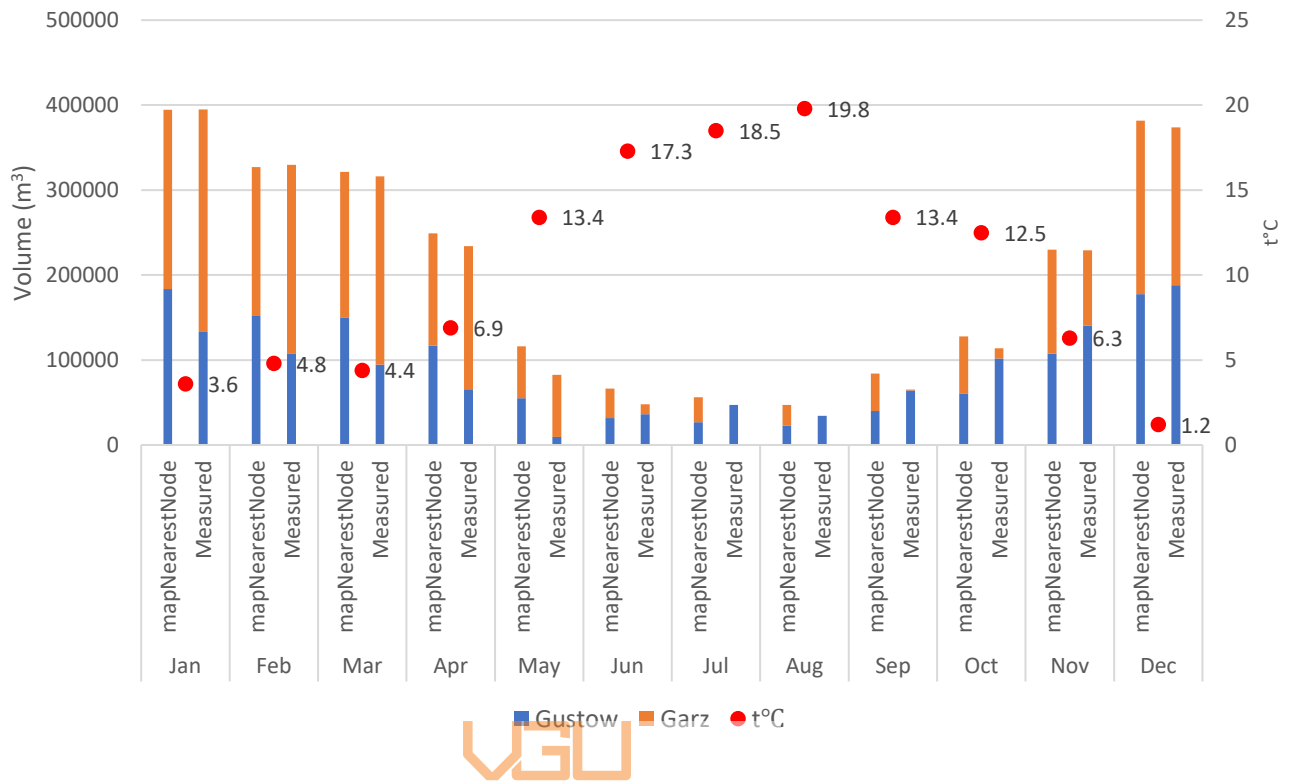


Figure 10: Absolute volume of Gustow–Garz section by mapNearestNodes & regulator measurements

Figure 11 visualizes the volume distribution obtained by aggregating volume consumption to exit point, STANET simulation with the input monthly average injection pressure obtained from measurements, and temperature and measured volume. The green line in the diagram marks the volume distribution derived from the equally weighted nodes method.

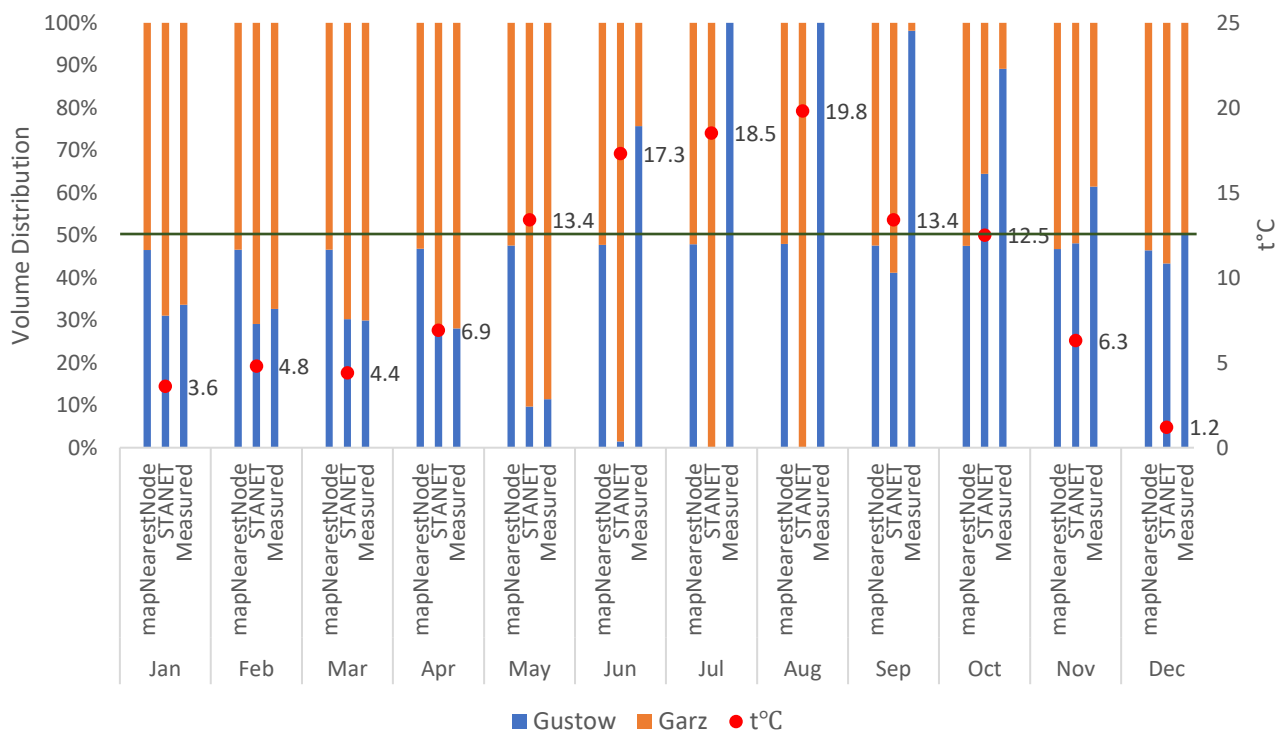


Figure 11: Volume distribution of Gustow – Garz section by mapNearestNodes & STANET &



Vietnamese-German University

The volume distribution for all months, except June to November, closely aligns with the measured volume, with the maximum difference at 6.96% observed in December. However, the distribution from mapNearestNodes significantly misaligns with the two methods for most of the year, except for November and December.

During November, the monthly average injection pressure at both regulators is recorded at 1.802 bar, and in December, the recorded monthly average temperature is 1.2 °C, considered to be low. These two months highlight that the volume distribution obtained from the mapNearestNode tool is relatively accurate under equal pressure and low-temperature scenarios.

Between June and October, despite the injection pressure at Garz regulator remained higher than Gustow regulator, the flow distribution through the Garz regulator drastically decreased, and Gustow regulator solely supplied for the section during June and July, while in August and September, the volume flow through the Garz regulator came in presence but still dominated by the Gustow regulator. This event can be attributed to the grid operator manually shutting down the operation of

one regulator during these months and resuming its operation, as both regulators significantly contributed to the gas supply in the section in November.

From May to August, according to the result of STANET, Garz regulator predominantly or entirely supplies the entire section. During these months, the injection pressure at Garz regulator was recorded to be lower than the pressure at the Gustow regulator, as illustrated in Figure 12, comprised with the elevated temperatures. Garz regulator predominantly supplied the volume in the section. This behavior aligns with the observation in section 4.1.2 regarding the impact of temperature on pressure drops in the section and volume flow through regulators. As temperatures rose, the proportion of pressure level which surpassed the pressure at the Gustow regulator also increased, consequently impeding the flow through this inlet.

In November, despite having the similar average temperature as in April, the primary gas supply transitioned from the Garz regulator to Gustow. This shift was attributed to a change in the dominant injection pressure. In April, Garz was set at a higher pressure level, but in November, Gustow assumed this position.



These months have underscored the suboptimal performance of mapNearestNode under different pressure scenarios, particularly in high-temperature conditions or when there is a manual impact on regulator operation. While the injection pressures at regulators exhibit fluctuations and are not consistently identical, particularly in 2022, the daily difference in injection pressure has a mean value of 0.00575 bar and a maximum difference of 0.019 bar. As depicted in Figure 9, it already shown that, a 0.005 bar difference in injection pressure at “Gustow – Garz” at 20°C already leads to a special occurrence, where the lowest pressure in the section surpasses the lower injection level. While the mapNearestNodes tool, initially created for scenarios with uniform pressure conditions, demonstrates capability under such conditions, its limitations become evident in scenarios with varying pressure.

The volume distribution derived from the equally node weights has a similar result with the one derived from the mapNearestNodes tool, this can be accounted for the evenly distribution of customers in the “Gustow – Garz” section.

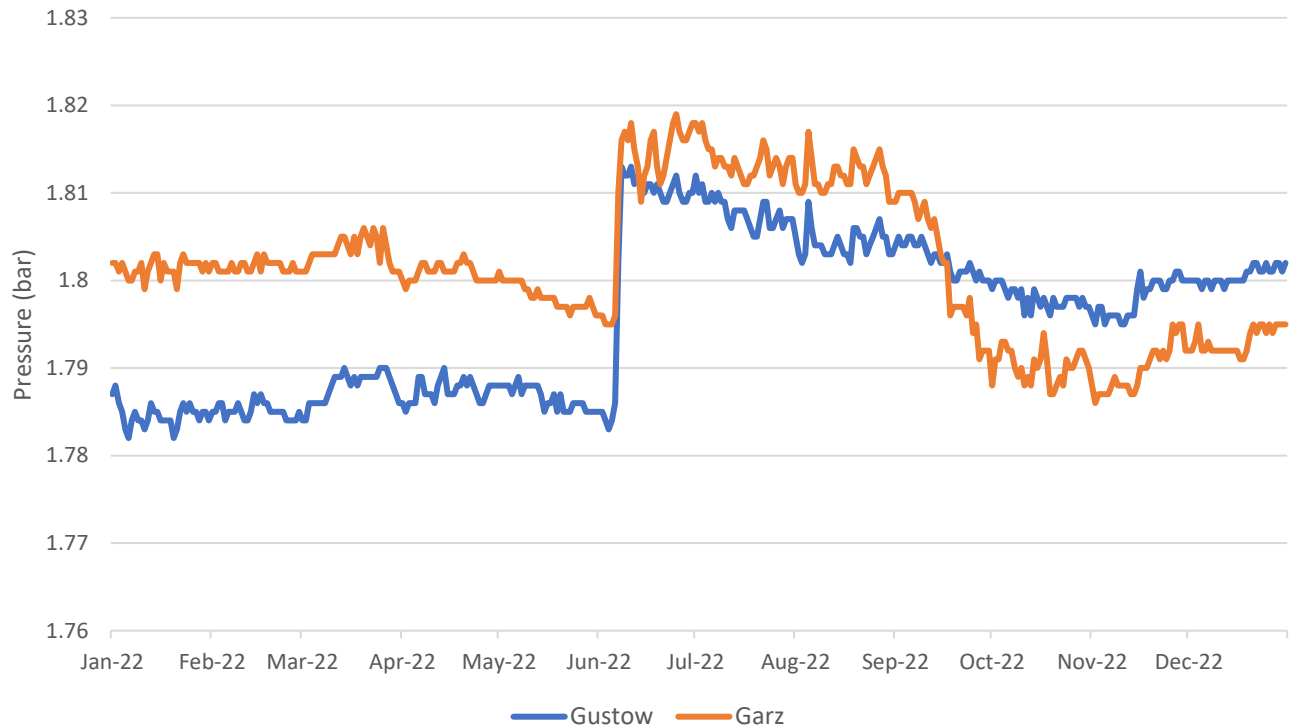


Figure 12: Daily pressure at Gustow and Garz regulators

Figure 13 illustrates the volume distribution at the same pressure ratio of 1.8 bar using the mapNearestNodes tool. This distribution closely resembles the static calculation of one hour obtained through STANET software, which were conducted at identical temperatures. Notably, the disparity between the two methods remains consistently below 10%. This, once again proves that equalizing the pressure of the two regulators mitigates the impact of temperature on volume distribution. Despite the monthly temperature fluctuations ranging from 1.2°C to 19.8°C throughout the year, the volume proportions calculated with STANET exhibit only minor variations.

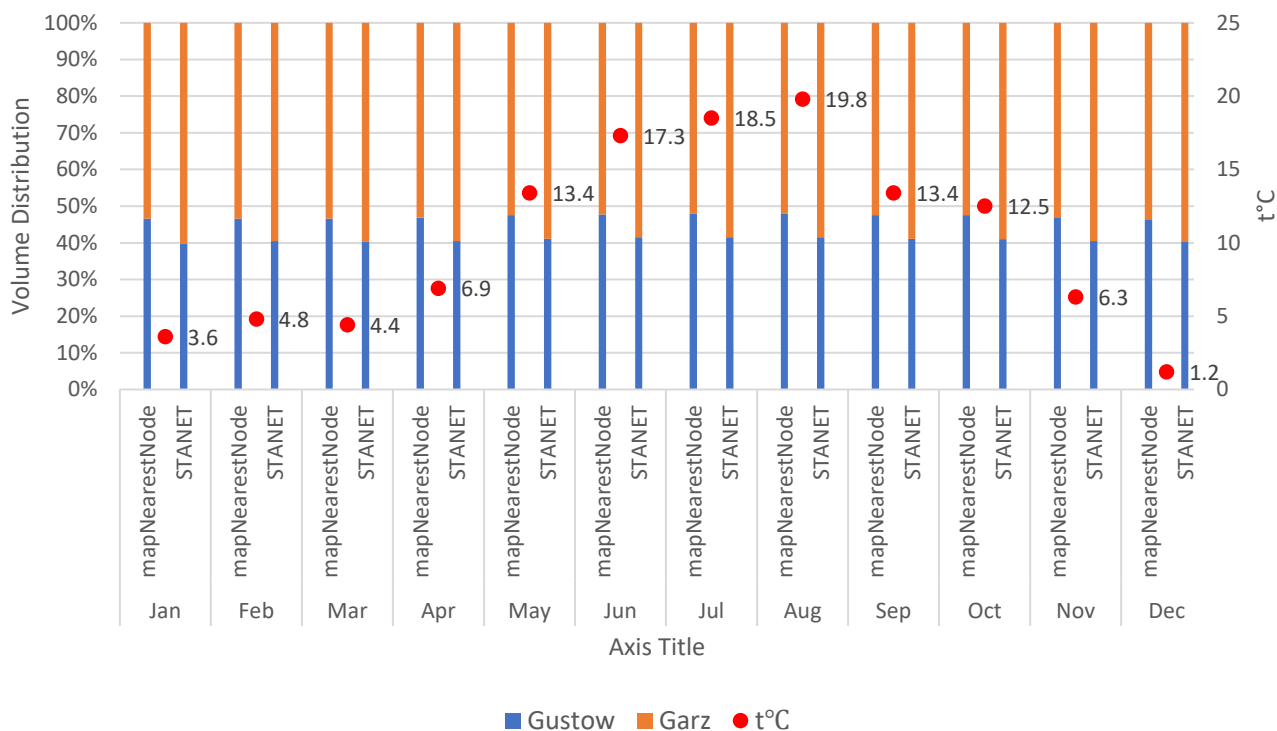


Figure 13: Volume distribution of Gustow–Garz section by mapNearestNodes & STANET at equal injection pressure (1.8 bar)

Figure 14 illustrates the SLP volume distributions of the “Northern Coastal” section derived from the allocation of the mapNearestNodes. Results are obtained from different sources, first is the volume obtained from the calculation with SmartSim, second one is the distribution derived from the dynamic node weights method they are both taken into comparison with the equally weighted nodes method. Additionally, the dynamic node weights were initially derived in daily resolution, the distribution value shown in the diagram is the monthly averaged from the daily node weights.

It is noted that the volume proportion derived from equally weighted methods differs from the others. On the other hand, the volume distribution obtained through dynamic node weights closely aligns with the simulated volume. Dynamic node weights also address the effect of SLP profiles mentioned in 4.1.1. This performance is affirmed by the proportion of Mukran, the special exit node in this section with a high share of the bakery profile (BA4). Obtained by dynamic node weights, it closely follows the distribution acquired from the simulation volume, with the highest difference at

0.86% recorded in August. This accounts for a 9.42% relative difference when compared with the distribution calculated with the simulation volume.

Unlike the “Gustow – Garz” section, the equally distributed volume of “Northern Coastal” section significantly misaligned with other node weights methods.

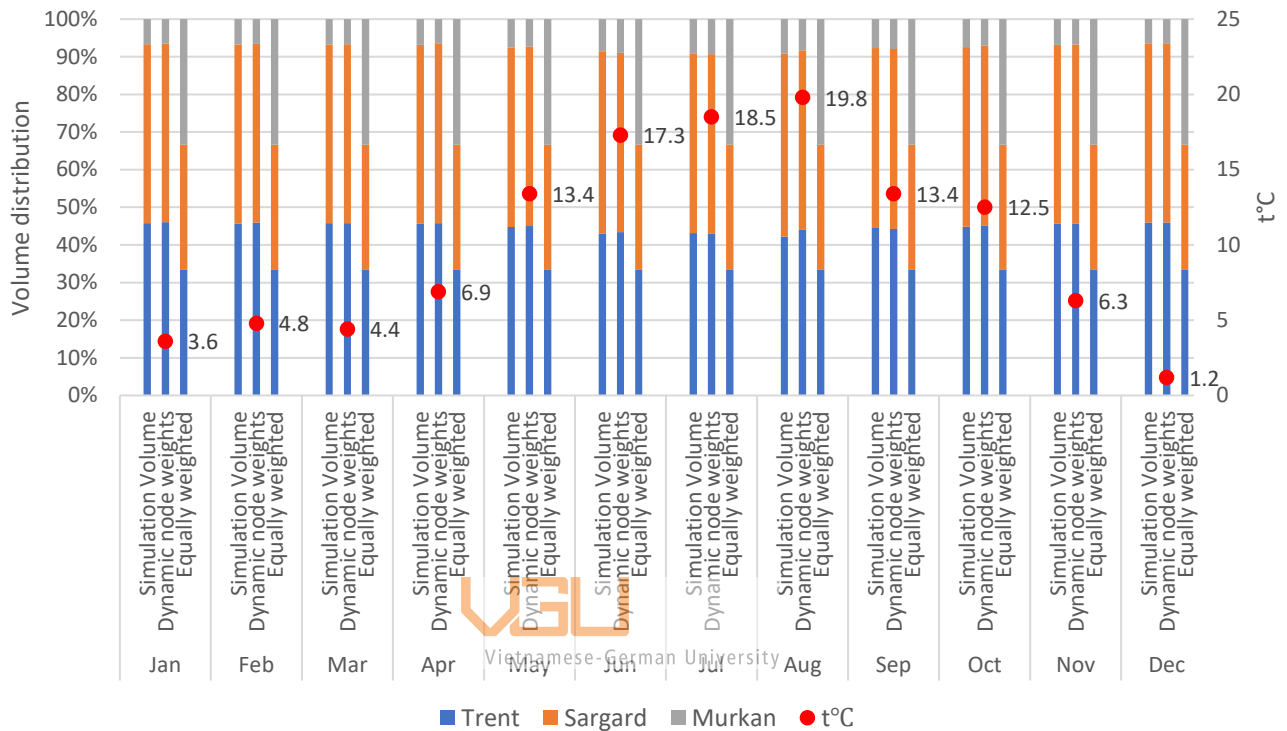


Figure 14: Volume distribution from SmartSim, dynamic node weights, and equally weighted nodes

4.3. Derivation of node weights

The methodology section 3.2 have mentioned three alternative methods of deriving node weights, the equally weighted nodes, fixed node weights derived from the volume distribution obtained through various measurement and simulations, and dynamic node weights estimated with the SLP methods and allocation with the mapNearestNodes tool. Based on the project- specification, not all methods are applicable. For the measured volume, its availability is inconsistent in various projects, and the information of the lower pressure grid, which is used to allocate customers to exit points with mapNearestNodes and set up static simulation of the section are available in all projects.

In the majority of projects, the measured volume is unavailable. However, when the measured volume is provided and its measurement quality is confirmed, it can simplify the volume distribution process in the section. This is because it can be directly employed to distribute volume to regulators, eliminating the necessity for additional procedures.

In the absence of measurement devices at inlets to the section, under the assumption that the assumption that temperature and consumption trends remain stable in subsequent years, fixed node weights can be determined from the volume distribution of the reference year.

One source of reference for volume distribution to establish node weights is by simulating the lower – pressure grid with STANET. The static simulation of the lower pressure grid using STANET is characterized by flexibility, allowing adjustments for various factors such as date, time, regulator injection pressure, and environmental temperature. It is proven with Figure 13 that, the volume distribution calculated with STANET aligns closely with the measured volume, which make STANET to be a reliable reference for setting up node weights. However, it's essential to note that the STANET simulation was conducted with hourly resolution, influenced by the hourly and daily factors of SLP profiles. While the effect was trivialized due to the high share of household profiles in “Gustow – Garz” for the higher share of different profiles, more details in 7.2, the result may be affected. Moreover, considering the flexibility in inputting pressures and temperatures for simulation, the volume distribution may become overly specific. Hence, fixed node weights obtained by STANET should be calculated based on monthly average input for pressure and temperature to mitigate this specificity. Furthermore, these weights should be reassessed when there are significant alterations in injection pressure and temperature trends.

The mapNearestNodes tool serves as an alternative source for establishing fixed node weights if the STANET model of sub – grids are not available. It demonstrates competence under uniform injection pressures but is susceptible to errors in different injection pressure scenarios, particularly in high-temperature conditions. Fixed node weights obtained through this method are also vulnerable

to the impact of SLP profiles when the temperature trend undergoes significant changes, as discussed in section 4.1.1.

In scenarios where RLM customers are not present, deriving dynamic node weights based on the allocation of customers via the `mapNearestNodes` tool and the SLP method yields similar distribution results to counterparts that use simulation volume to establish fixed node weights. Additionally, node weights derived from this method demonstrate the capability to address the influences of SLP profiles on volume distribution under various temperature conditions. Furthermore, node weights established through this method can be derived solely from the allocation results, eliminating the necessity for additional simulations.

Overall, if the availability and reliability of the measured volume is guaranteed, it becomes the most appropriate reference to distribute volume into the section without the need of establishing node weights. The static simulation of the section with STANET also proves to be a reliable reference in case the STANET model for the sections is accessible. The `mapNearestNodes` tool demonstrates its capability under the assumption of uniform injection pressures, offering results that can be used for deriving fixed node weights through simulation or dynamic node weights in the absence of RLM customers. In situations where alternative methods are not accessible, equally weighted node weights can be employed. While acknowledging their susceptibility to errors due to the distribution of volume through regulators are not always equal, it stands out as the most effortless method for volume distribution when measurement data is unavailable.

However, when employing the `mapNearestNodes` tool to allocate customers to exit points, the tool itself also exhibits some fallacies. As previously mentioned, the `mapNearestNodes` tool exhibits limitations under conditions of unequal pressures. Conversely, under circumstances of uniform pressure, the aggregated customer consumption derived from the `mapNearestNodes` tool aligns with the calculation results obtained through STANET. However, real-world scenarios often entail fluctuating and not precisely known pressures at the regulators. This variance in regulator

pressures, particularly in high temperature conditions, significantly influences the volume distribution within the section.

The mapNearestNodes tool presents a second limitation by mapping customers to the single exit node. Figure 15 displays the volume flow to the sub-grid through the Gustow and Garz regulators under equal pressure conditions, obtained by incorporating the sub-grid into the SmartSim calculation. The yellow area denotes the region exclusively supplied by the Gustow regulators, the blue area designates the area solely served by the Garz regulator, and the green area signifies the region supplied by both regulators. This delineation was determined by analyzing the monthly average flow rate and direction through the pipes. At the border of the supply area regulated by a single regulator, the flow rate approaches zero. In this simulation, both the flow from Garz and Gustow is directed toward the green area. These areas remain constant throughout 2022 under uniform pressure injection setups simulated with SmartSim.

The occurrence of customers drawing gas from both regulators is also expected from RLM customers exhibiting high consumption, which can potentially affect the network and draw gas from multiple regulators. Therefore, the procedure of mapping the customers, especially RLM customers to one exit point is questionable.

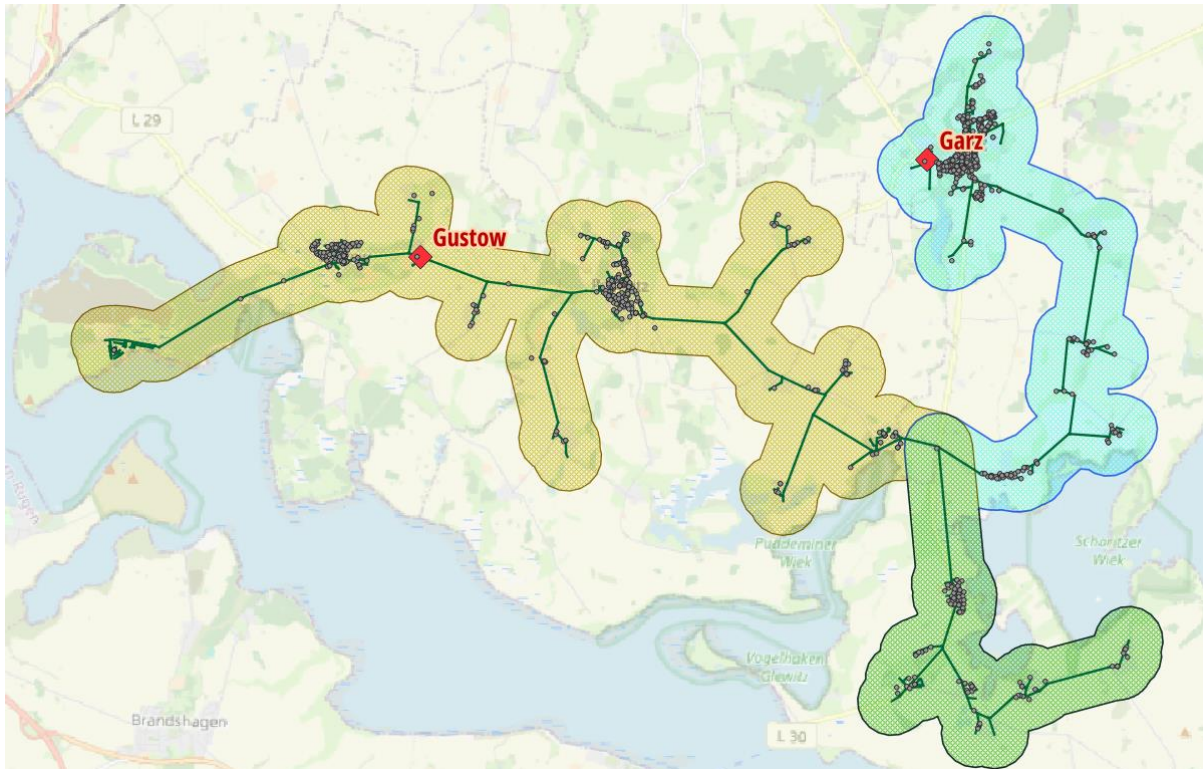


Figure 15: Area supplied by Gustow, Garz regulators at same pressure

Allocating to a single exit point becomes susceptible to errors, particularly when two or more exit points are situated in close proximity. This situation is exemplified by “Prora” and “Binz Heizkraftwerk” in the “Central” section, as illustrated in Figure 16 about the section and regulator positions.

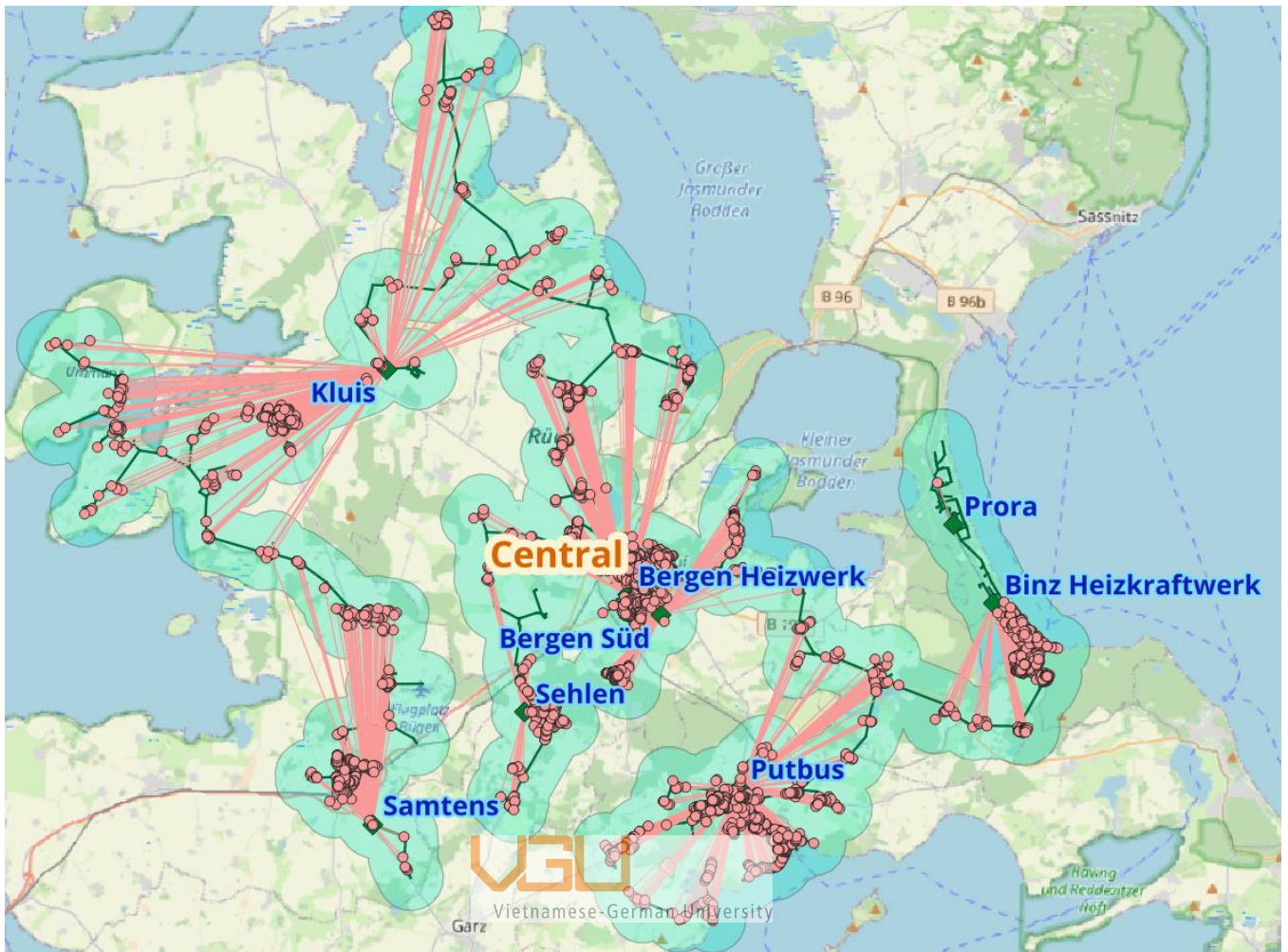


Figure 16: Rügen central section

Figure 17 shows the volume flow through these exit points, the customers gas consumption aggregated by the mapNearestNodes tool aligns with the total volume flow measured by measurement devices at these exit points. This concordance suggests that these two regulators are intended to collectively supply gas to a specific area. However, notable disparities arise when examining the individually calculated volumes assigned to each exit point in comparison to the measurements. This discrepancy can be attributed to the close proximity of the two exit points, both designed to supply gas to the same area. The mapNearestNodes tool, in its customer allocation process, only assigns customers to a singular exit point, contributing to the observed differences in calculated volumes as opposed to the measured values.

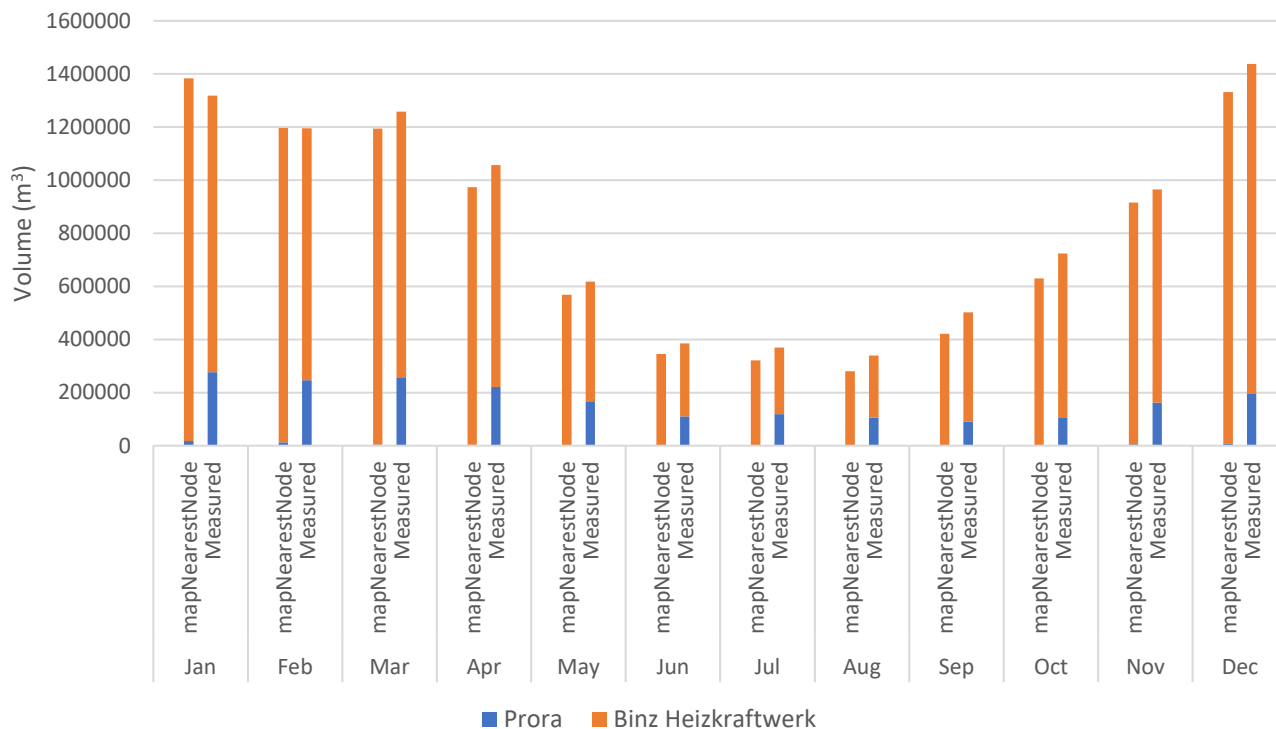


Figure 17: Volume flow through Prora and Binz Heizkraftwerk regulators

Another limitation in the operation of the `mapNearestNodes` tool is its disregard for the capacity constraints of regulators. In scenarios where multiple regulators are assigned to supply a specific area, the tool may aggregate consumption values that exceed the capacity of the regulator.

Overall, the output produced by the `mapNearestNodes` tool is prone to errors stemming from three primary factors. Firstly, its performance is compromised under conditions of unequal pressures, particularly in high-temperature scenarios, affecting the accuracy of the allocation results. The second limitation arises from the tool's approach of allocating customers to a single exit node, introducing errors when managing exit points in close proximity or when dealing with customers or groups drawing gas from multiple inlet points. Additionally, the tool overlooks the flow capacity of regulators, potentially resulting in the aggregation of more volume than the regulator can handle.

5. Summary and Outlook

The thesis covers two main subjects, setting up a SmartSim topology from given GIS data and examining how the distribution of volume in sub-grids can be modelled for simulations with SmartSim. For the latter the idea of using fixed weighing factors so called node weights is evaluated and discussed.

The first subject is to establish a procedure for creating a graph model to be used as a SmartSim topology. In addition to the human evaluation involved in this process, the procedure incorporates the automation of repetitive steps using the QGIS Python console and thus reduces the manual effort when setting up a topology. The topology of the Rügen grid created by this procedure is used for the evaluation of the second subject.

For the second subject the volume distribution in areas of the grid that are determined as downstream grids while creating the graph model and which have multiple injection points are analyzed. The background is that the volume distribution in these downstream grids is most often not measured but has an important influence on the calorific value calculated for these grid parts. To model the volume distribution one idea is to use node weights that under the assumption that the consumption trends remain relatively stable in the subsequent years once been derived can be used for multiple years.

To evaluate the idea of using node weights it is analyzed which factors influence the volume distribution within a section. Firstly, it is shown that the distribution of SLP profiles has an effect on the distribution of volume. The SLP profiles associated with cooking gas (HK3), bakery (BA4), and laundry services (WA4) demonstrate consistent demands for gas. These profiles maintain higher consumption levels compared to others during temperature increases, without experiencing a significant rise during temperature decreases. This behavior contributes to a notable shift in the volume distribution at exit points, characterized by a high share of these profiles when temperatures vary.

Secondly, the effects of temperature and injection pressure on volume distribution are explored in a sensitivity analysis with STANET. Temperature, directly affecting gas consumption demands, has a pivotal role in influencing the pressure drop across the grid. At instance when the injection pressured are injecting regulators are different, comprised with the low-pressure drop attributed to low consumption, leads more part of the section where pressure surpasses the lower injection pressure thus blocks the flow from the regulator to these areas. In contrast, under equal pressure ratios, the effect of temperature on volume distribution is neglectable.

Additional to the evaluation of influence factors on the volume distribution, a comparison between different ways of modelling the volume distribution is conducted on the “Gustow – Garz” section of the Rügen grid. This comparison includes the measured volume provided by the grid operator as a reference, the volume distribution from STANET’s static simulation of the lower pressure grid, and the aggregated volume consumption to the nearest exit point using the mapNearestNodes tool. The comparison is used to discuss the usage of node weights.

The usage of node weights depends on the data a grid operator can provide. As mentioned, it is uncommon for volume measurements at regulators to be provided, and the availability of the STANET model of sections is also not universal across projects. In certain projects, the information pertaining to the lower-pressure grid may not be provided, thereby eliminating options for utilizing mapNearestNodes or conducting STANET simulations.

Reliable measurements can be utilized to distribute volume to exit points directly without the necessities of other procedures. The STANET simulation, when accessible, has shown consistent alignment between simulated and measured volumes on a monthly resolution at “Gustow – Garz” section. However, it failed to match with the months from June to October due to manual flow adjustment of the grid operator. In reality, the pressure at regulators may not consistently be set at a precise value and could undergo alterations after maintenance procedures, this potentially result in significant changes in volume distribution. Thus, it is necessary to inspect the injection pressure, manual operations and consider reevaluating node weights before employing them.

The mapNearestNodes tool has similar results as derived from STANET when the injection pressures of the section are uniform. For the section “Gustow - Garz” the volume distribution doesn’t align with the measured volumes as good as the one from STANET, though. The influence of different injections pressures, particularly when temperatures are high, is an explanation why. This effect is unaccounted for when employing the mapNearestNodes tool, in contrast to STANET. It is evident that mapNearestNodes tool has its limitations when injections pressures vary. Additionally, utilize the allocation of the mapNearestNodes tool, in the absence of RLM customers, dynamic node weights derived from SLP methods shares the similar volume distribution with the fixed node weight counterpart derived from calculation while being responsive to temperature without the necessities of simulation. Node weights derived from the mapNearestNodes tool have proven effective under uniform injection pressure in the section. However, there are rooms for improvement in this procedure. The current exclusive allocation of customers to the nearest exit point poses challenges, particularly when multiple regulators are in close proximity. This approach also prompts questions about assigning all consumption of RLM customers to a single exit point instead of distributing it among all regulators in the area. To address this issue, the mapNearestNodes algorithm can incorporate a procedure specifically designed for these exit points, and implement a distinct allocation procedure for RLM customers. Furthermore, the capacity of the regulator should be taken into consideration. The mapNearestNodes tool's allocation performance is suboptimal, attributed to the oversight of unaccounted injection pressure and temperature factors. To enhance allocation results, the algorithm could be refined to incorporate input pressure and temperature in its design.

In the end, employing equally weighted nodes is a viable option. They are simple to set up, albeit less precise. While alternative methods may not consistently exhibit closer alignment with measured data, equally weighted nodes serve as a valid approach before discovering more advanced techniques. Despite their susceptibility to errors arising from unequal volume distribution through regulators, they stand out as the most straightforward method for volume distribution in cases where measurement data is unavailable.

6. Bibliography

- [1] D. G. M. S. Jaro Jens, "Market state and trends in renewable and low-carbon gases in Europe," Dec. 2021.
- [2] M. Hellwig, "Entwicklung und anwendung parametrisierter standard-lastprofile," Technische Universität München, München, 2003.
- [3] P. Schley, J. Schenk, and A. Hielscher, "Brennwertverfolgung in Verteilnetzen: Teil 1 – Entwicklung und Validierung des Verfahrens," *GWF Gas Erdgas*, vol. 152, no. 9, pp. 552–556, 2011.
- [4] Joachim Schenk, Peter Schley, and Andreas Hielscher, "Brennwertverfolgung in Verteilnetzen: Teil 2-Auswertung Feldversuch und Implementierung," *GWF Gas Erdgas*, vol. 10, no. 10, pp. 676–683, 2011.
- [5] Andreas Hielscher, Christian Fiebig, Roland Span, Peter Schley, and Joachim Schenk, "Brennwertverfolgung mit SmartSim - ein neuer Rechenkern zur Strömungssimulation," *GWF Gas Erdgas*, vol. 155, no. 10, pp. 736–743, 2014.
- [6] DVGW, "DVGW G 685-2 (A)," Aug. 2020.
- [7] A. Hielscher, *Ein neues Verfahren zur strömungstechnischen Simulation von Gasnetzen.*, 1st ed., vol. 505. in *Strömungstechnik*, vol. 505. Düsseldorf: VDI Verlag, 2017. doi: 10.51202/9783186505071.
- [8] Dirk Vollmer, "Ein Beitrag zur prozeßbegleitenden Zustandsbeobachtung in regionalen Erdgasverteilungsnetzen," Technischen Universität Clausthal, 1999.
- [9] C. FIEBIG, T. WEISER, and H. HÖPFNER, "Abschlussbericht Validierung : Gasbeschaffenheitsverfolgung mit SmartSim im Netzbereich „GLG- Süd-West“ der LSW Netz GmbH & Co. KG. 2020," 2020.
- [10] FORSCHUNGSGESELLSCHAFT FÜR ENERGIEWIRTSCHAFT MBH, *Statusbericht zum Standardlastprofil Gas*. München, 2014.

- [11] “Calculation of Gross Heating Value, Relative Density, Compressibility and Theoretical Hydrocarbon Liquid Content for Natural Gas Mixtures for Custody Transfer,” in *GPA Standard 2172-09 and API MPMS*, 3rd ed., 2009.
- [12] Bernd Geiger and Mark Hellwig, “Entwicklung von Lastprofilen für die Gaswirtschaft im Auftrag des Bundesverbandes der deutschen Gas- und Wasserwirtschaft e.V. und des Verbandes kommunaler Unternehmen e.V. Gewerbe, Handel und Dienstleistung,” TU München, München, 2002.
- [13] National Geographic Society, “GIS (Geographic Information System).”
- [14] J. R. , ed. Herring, “Simple Feature Access – Part 1: Common Architecture,” Open Geospatial Consortium.
- [15] NetworkX, “dijkstra_path_length,”
https://networkx.org/documentation/stable/reference/algorithms/generated/networkx.algorithms.shortest_paths.weighted.dijkstra_path_length.html.
- [16] G. Howell, “Darcy – Weisbach equation,” in *Aerospace Fluid Component Designers’ Handbook. Volume I, Revision D*, vol. 1, 1970, p. 87.

7. Appendixes

7.1. Appendix A: Create Graph Model with QGIS Python Console

Libraries used:

```
import os
from qgis.core import *
```

Functions:

```
def set_up_folder(pipe_input):
# 2 extra folders are created
# Temp folder to store all the shape files in process
# Out to store the result pipe and node shape file
    data_dir = '/' .join(pipe_input.split('\\')[:-1])
    temp_dir = f"{data_dir}/Temp"
    out_dir = f"{data_dir}/Out"
    os.makedirs(temp_dir, exist_ok = True)
    os.makedirs(out_dir, exist_ok = True)
    return temp_dir, out_dir
```

```
def create_node_layer(pipe_input, vertices_output, node_output_1, node_output_2):
#A new blank node layer is created with this function
#Extract Start/End Vertex of pipes
#REF: 28.1.22. Vector geometry — QGIS Documentation documentation
    processing.run(
        "native:extractspecificvertices",
        {'INPUT': pipe_input,
         'VERTICES': '0,-1',
         'OUTPUT': vertices_output})
#Delete Duplicate Geometries
#REF: 28.1.21. Vector general — QGIS Documentation documentation
    processing.run(
        "native:deleteduplicategeometries",
        {'INPUT': vertices_output,
         'OUTPUT': node_output_1})
#Drop all fields in Node Layer
#REF: 28.1.25. Vector table — QGIS Documentation documentation
    layer = QgsVectorLayer(node_output_1)
    field_names = [field.name() for field in layer.fields()]
    processing.run(
        "native:deletecolumn",
        {'INPUT': node_output_1,
         'COLUMN': field_names,
         'OUTPUT': node_output_2})
```

```

def adding_node_attributes(node_input, NodeID ,precision = 3):
#Node ID, X coordinate, Y coordinate, WKT of node is created
#Add new field
layer = QgsVectorLayer(node_input)
pr = layer.dataProvider()
fields_arr = [
(NodeID,QVariant.String),
("X",QVariant.String),
("Y",QVariant.String),
("wkt",QVariant.String)]
for i in fields_arr:
    if i[0] not in [fld.name() for fld in layer.fields()]:
        pr.addAttributes([QgsField(i[0],i[1])])
        layer.updateFields()
        print(i[0] + ' is added to the node layer')
#Add context to features
exp_arr = [
(NodeID,"'K_' || @id"),
("X","$x"),
("Y","$y"),
("wkt",f"right(geom_to_wkt(@geometry,{precision}),length(geom_to_wkt(@geometry,{
precision}))-strpos( geom_to_wkt(@geometry,{precision}),'(')+1)")]
#Add context to features
context = QgsExpressionContext()
context.appendScopes(QgsExpressionContextUtils.globalProjectLayerScopes(layer))
with edit(layer):
    print("Generating Node's Attributes...")
    for f in layer.getFeatures():
        context.setFeature(f)
        for i in exp_arr:
            f[i[0]] = QgsExpression(i[1]).evaluate(context)
            layer.updateFeature(f)
    print("Node's Attributes Generated")

```

```
def add_pipe_attributes(pipe_input, precision = 3):
#Start_wkt, End_wkt,Length of pipe is created
    layer = QgsVectorLayer(pipe_input)
    pr = layer.dataProvider()
    #Necessary Attributes
    fields_arr = [
        ("Start_wkt",QVariant.String),
        ("End_wkt",QVariant.String),
        ("Length",QVariant.String)
    ]
    #Field Expression
    exp_arr = [
        ("Start_wkt",f"right(geom_to_wkt(start_point(@geometry),{precision}),length(
geom_to_wkt(start_point(@geometry),{precision}))- strpos(
geom_to_wkt(start_point(@geometry),{precision}),'')+1)"),
        ("End_wkt",f"right(geom_to_wkt(end_point(@geometry),{precision}),length(geom
_to_wkt(end_point(@geometry),{precision}))- strpos(
geom_to_wkt(end_point(@geometry),{precision}),'')+1)"),
        ("Length", "$length")]
    for i in fields_arr:
        if i[0] not in [fld.name() for fld in layer.fields()]:
            pr.addAttributes([QgsField(i[0],i[1])])
            layer.updateFields()
            print(i[0] + ' is added to the pipe layer')
    #Add context to features
    context = QgsExpressionContext()
    context.appendScopes(QgsExpressionContextUtils.globalProjectLayerScopes(layer))
    with edit(layer):
        print("Generating Pipe's Attribute...")
        for f in layer.getFeatures():
            context.setFeature(f)
            for i in exp_arr:
                f[i[0]] = QgsExpression(i[1]).evaluate(context)
            layer.updateFeature(f)
        print("Pipe's Attribute Generated")
```

```
def map_node_to_pipe(pipe_input, node_input, pipe_ouput_1, pipe_ouput_2):  
#Node ID is mapped to Pipe Start Node ID and Pipe End Node ID  
#Map Start Node  
#REF: 28.1.21. Vector general — QGIS Documentation documentation  
processing.run(  
"native:joinattributetable",  
{'INPUT': pipe_input, 'FIELD': 'Start_wkt',  
'INPUT_2': node_input, 'FIELD_2': 'wkt',  
'FIELDS_TO_COPY': ["Node ID"],  
'METHOD': 1,  
'DISCARD_NONMATCHING': False,  
'PREFIX': 'Start ',  
'OUTPUT': pipe_ouput_1})  
#Map End Node  
processing.run(  
"native:joinattributetable",  
{'INPUT': pipe_ouput_1, 'FIELD': 'End_wkt',  
'INPUT_2': node_input, 'FIELD_2': 'wkt',  
'FIELDS_TO_COPY': ["Node ID"],  
'METHOD': 1,  
'DISCARD_NONMATCHING': False,  
'PREFIX': 'End ',  
'OUTPUT': pipe_ouput_2})  
print('Node IDs is mapped to pipes')
```


Main:

```

#By in putting shape file of the pipe layer, a pipe layer in SmartSim topology
format is created
#An extra node layer is created if a node layer is not provided
if __name__ == '__console__':
    precision = 3 #Precision to decimal places
    node_exist = 1 #Is node layer available? 1 for 'Yes' 0 for 'No'
    node_ID = "Node ID" # Desired name for Node ID
    pipe_input = r"D:\QGIS Python Console\pipe.shp" #Input pipe shape file
    temp_dir,out_dir = set_up_folder(pipe_input = pipe_input)
    if node_exist == 0:
        create_node_layer(
            pipe_input = pipe_input,
            vertices_output = f"{temp_dir}/vertices.shp",
            node_output_1 = f"{temp_dir}/node_raw.shp",
            node_output_2 = f"{out_dir}/node.shp")
        adding_node_attributes (
            node_input = f"{out_dir}/node.shp",
            NodeID = "Node ID",
            precision = precision)
        add_pipe_attributes (
            pipe_input = pipe_input,
            precision = precision)
        map_node_to_pipe(
            pipe_input = pipe_input,
            node_input = f"{out_dir}/node.shp",
            pipe_ouput_1 = f"{temp_dir}/pipe_temp.shp",
            pipe_ouput_2 = f"{out_dir}/pipe.shp")
    else:
        #path to Node_layer
        node_input = r"D:\QGIS Python Console\node.shp" #Input pipe shape file
        node_input = node_input.replace('\\', '/')
        adding_node_attributes(
            node_input = node_input,
            NodeID = "Node ID",
            precision = precision)
        add_pipe_attributes(
            pipe_input = pipe_input,
            precision = precision)
        map_node_to_pipe(
            pipe_input = pipe_input,

```

7.2. Appendix B: Rügen SLP profiles and their distribution in analyzed section

Profile ID	Profile type
BA4	Bakery
BD4	Other Services
BEF	Single Family House
BH4	Accommodation
BMF	Multi Family House
GA4	Restaurant
GB4	Gardening
HA4	Commerce
HK3	Cooking gas
KO4	Local Authority/ Bank/ Non-profit Organization
MF4	Household-like Businesses
MK4	Metal and Motor Vehicles
PD4	Printing Service
WA4	Laundry Service

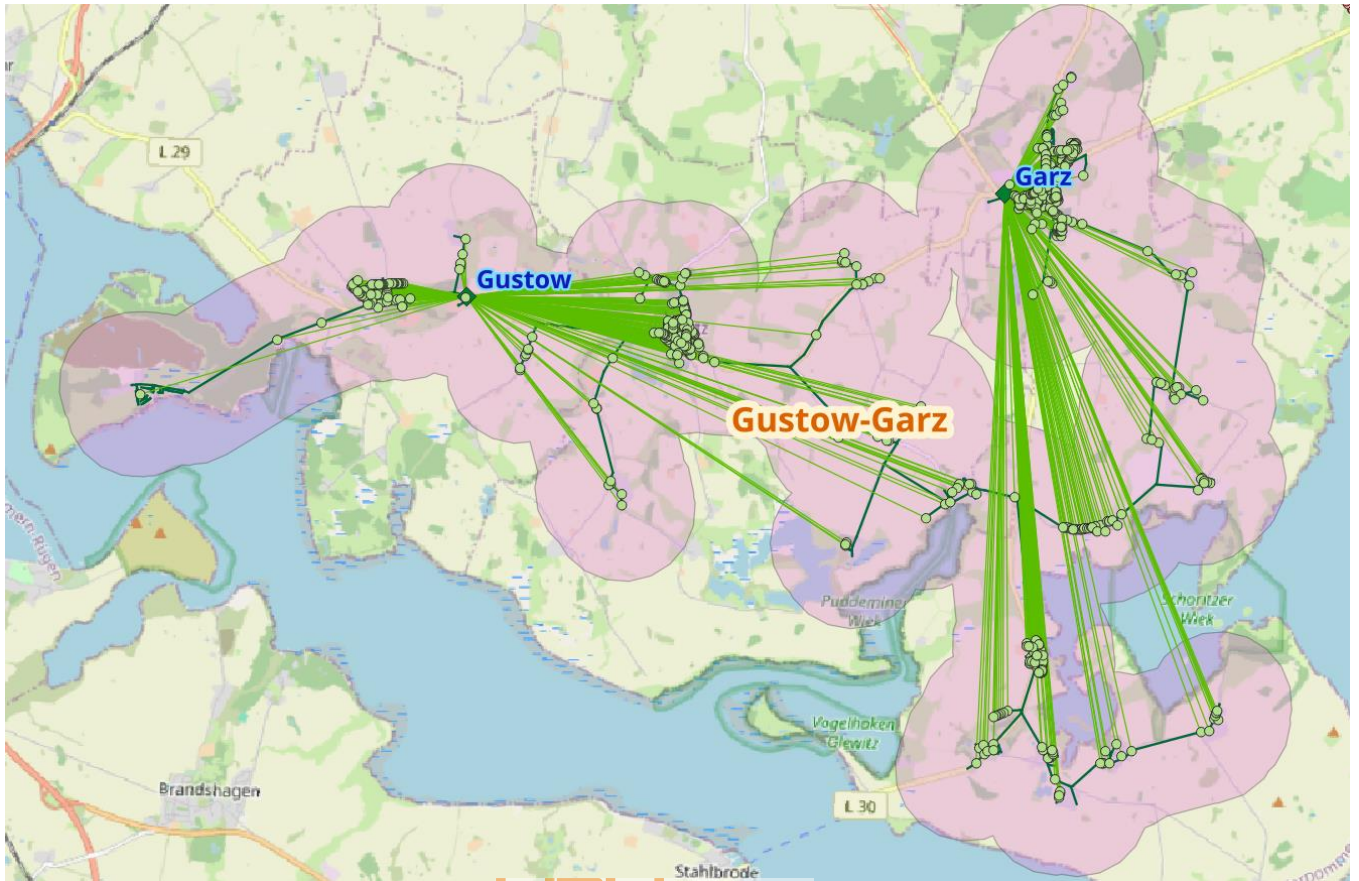


Figure 18: Gustow - Garz section

Vietnamese-German University

	BA4	BD4	BEF	BH4	BMF	GA4	GB4	HA4	HK3	KO4	MF4	MK4	PD4	WA4
Gustow	-	0.03	0.67	0.06	0.17	0.01	-	0.02	-	0.02	0.01	-	-	-
Garz	-	0.01	0.67	0.03	0.08	0.01	0.01	0.01	-	0.12	0.05	-	-	-

Table 2: SLP profile ratios allocated to Gustow – Garz exit points

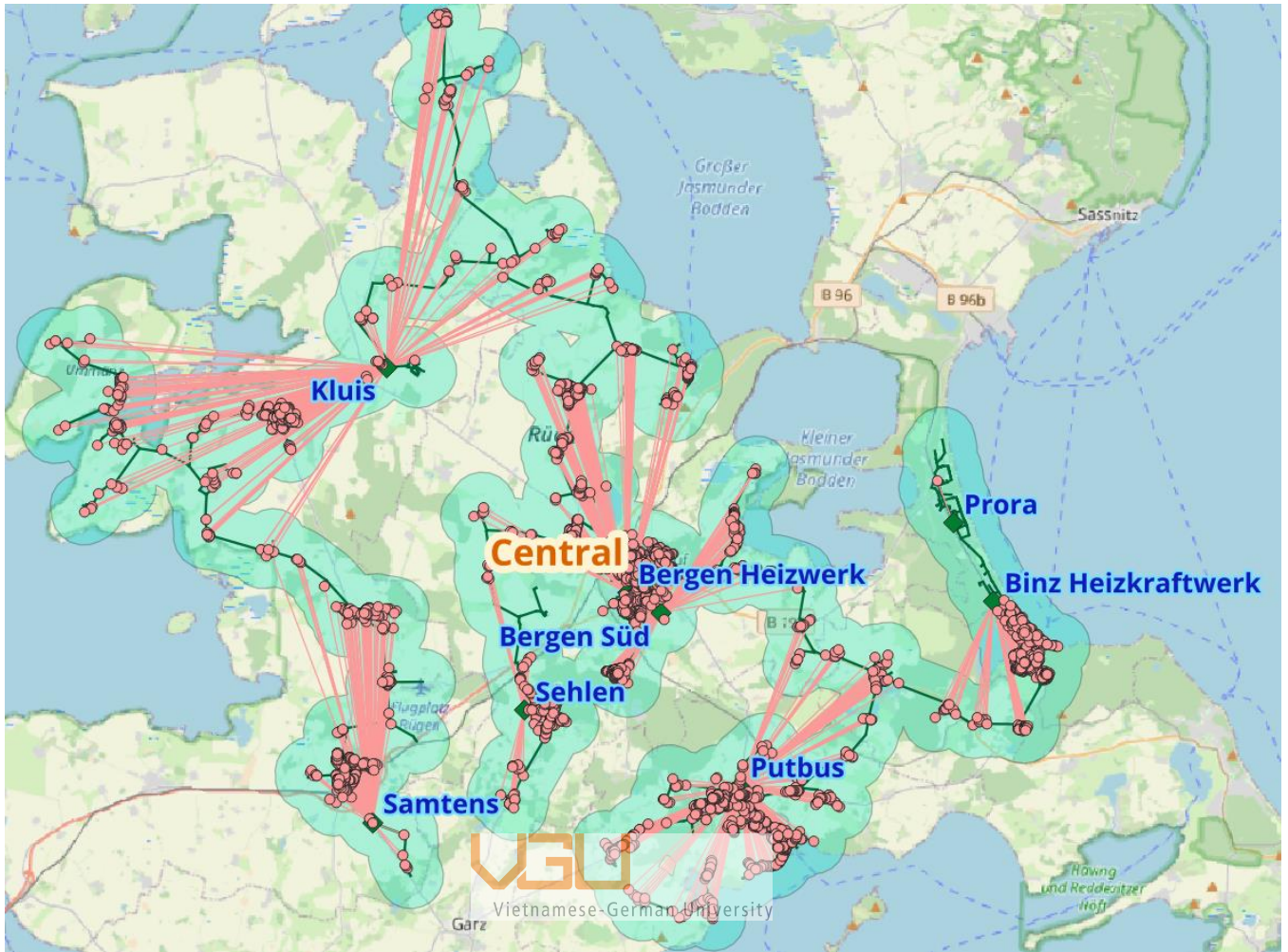


Table 3: Central section

	BA4	BD4	BEF	BH4	BMF	GA4	GB4	HA4	HK3	KO4	MF4	MK4	PD4	WA4
Samtens	-	0.13	0.59	0.03	0.09	0.01	-	0.05	-	0.03	0.06	0.01	-	-
Kluis	-	0.01	0.56	0.10	0.20	0.05	-	0.03	-	0.02	0.03	-	-	-
Sehlen	-	0.02	0.75	0.06	0.10	0.04	-	0.03	-	0.01	-	-	-	-
Bergen HW	0.01	0.04	0.44	0.05	0.16	0.06	-	0.12	-	0.08	0.01	0.02	-	-
Bergen Süd	0.02	0.14	0.56	0.03	0.07	-	-	0.09	-	0.08	0.01	0.02	-	-
Putbus	-	0.02	0.58	0.07	0.17	0.05	-	0.01	-	0.04	0.04	-	0.01	-
Prora	-	-	-	-	1.00	-	-	-	-	-	-	-	-	-
Binz HKW	0.00	0.01	0.2	0.23	0.34	0.11	-	0.02	-	0.03	0.04	0.01	-	0.01

Table 4: SLP profile ratios allocated to Central exit points

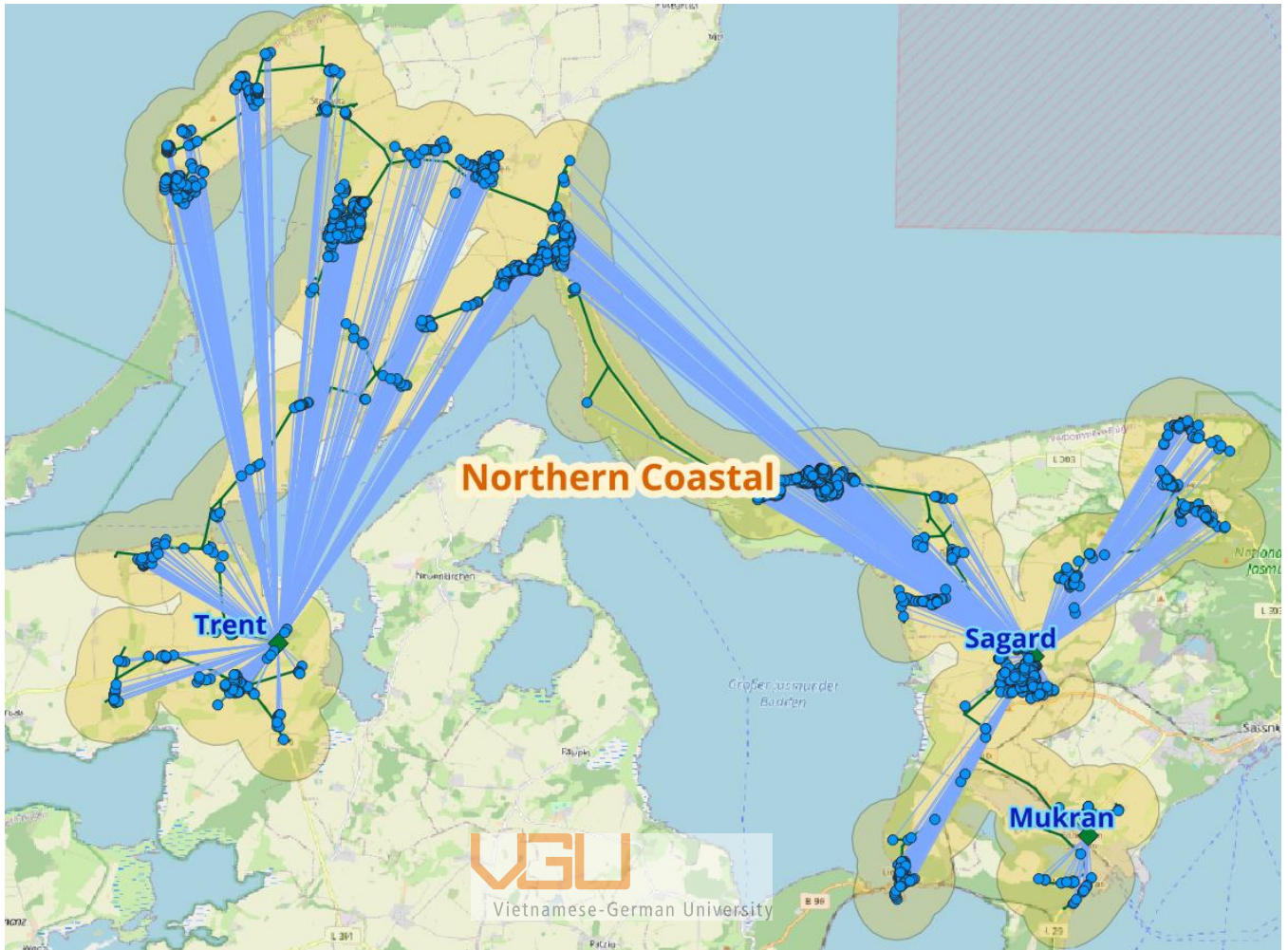


Table 5: Northern Coastal section

	BA4	BD4	BEF	BH4	BMF	GA4	GB4	HA4	HK3	KO4	MF4	MK4	PD4	WA4
Trent	-	0.04	0.56	0.14	0.15	0.04	0.00	0.02	-	0.03	0.02	0.00	-	-
Sargard	0.00	0.02	0.51	0.18	0.18	0.04	-	0.03	-	0.02	0.01	0.00	-	0.00
Mukran	0.15	0.12	0.50	0.11	0.07	0.05	-	0.01	-	0.00	-	-	-	-

Table 6: SLP profile ratios allocated to Northern Coastal exit points

7.3. Appendix C: SLP & RLM volume shares in Rügen' sections

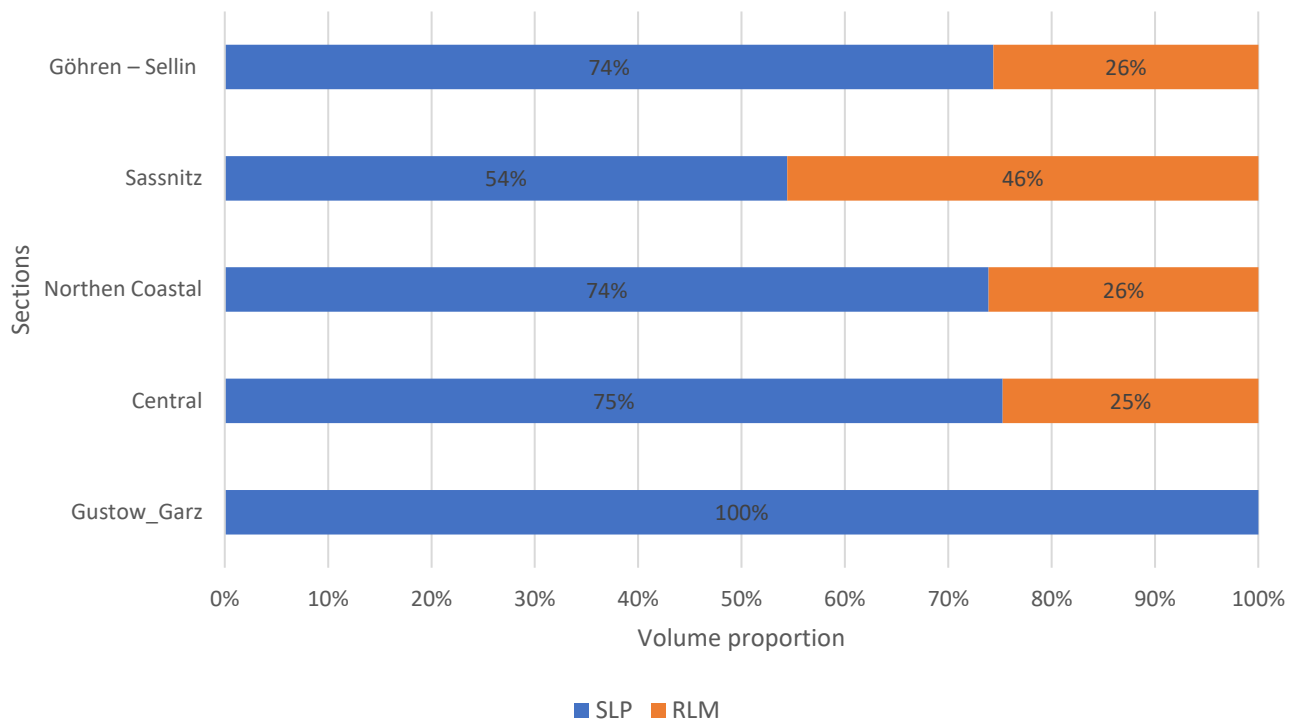


Figure 19: SLP & RLM volume shares in Rügen' sections in 2022